OAK RIDGE NATIONAL LABORATORY
operated by
UNION CARBIDE CORPORATION
NUCLEAR DIVISION
for the
U.S. ATOMIC ENERGY COMMISSION

ORNL-TM-2253

COPY NO. -

DATE - November 18, 1968

Neutron Physics Division

NEUTRON AND PROTON SPECTRA FROM TARGETS BOMBARDED BY 450-MeV PROTONS+

J. W. Wachter, W. A. Gibson,* and W. R. Burrus*
Oak Ridge National Laboratory, Oak Ridge, Tennessee

Abstract

The energy spectra of secondary neutrons in the energy region between 100 and 450 MeV emitted by targets bombarded by 450-MeV protons were measured using a proton recoil spectrometer. Secondary proton measurements were also made with this spectrometer. The measurements were made on Be, C, Al, Cu, Co, Pb, and Bi targets and at several angles between 0 and 60°. Two general target thicknesses were employed: thin targets in which the primary beam lost little energy and in which further interaction of the secondary particle was small, and thick targets in which the primary beam lost all or a significant fraction of the initial energy and in which the probability of the secondary particles undergoing further interaction was large. The thin-target results are expressed as cross sections and the thick-target results represent a nucleon transport and are expressed as a yield.

N70-78024
(ACCESSION NUMBER) (THRU)
53 (PAGES)
CR-110462 (NASA CR OR TMX OR AD NUMBER)
(CODE) (CATEGORY)
FACILITY FORM 602

NOTE: This work partially supported by NATIONAL AERONAUTICS AND SPACE ADMINISTRATION under Order R-104(1).

NOV 1970
RECEIVED
NASA STI FACILITY
INPUT BRANCH

FEB 1969
RECEIVED
NASA STI FACILITY
INPUT BRANCH

+Submitted for journal publication.

*Now with Tennecomp, Oak Ridge, Tennessee.

NOTICE This document contains information of a preliminary nature and was prepared primarily for internal use at the Oak Ridge National Laboratory. It is subject to revision or correction and therefore does not represent a final report.

LEGAL NOTICE

This report was prepared as an account of Government sponsored work. Neither the United States, nor the Commission, nor any person acting on behalf of the Commission:

A. Makes any warranty or representation, expressed or implied, with respect to the accuracy, completeness, or usefulness of the information contained in this report, or that the use of any information, apparatus, method, or process disclosed in this report may not infringe privately owned rights; or

B. Assumes any liabilities with respect to the use of, or for damages resulting from the use of any information, apparatus, method, or process disclosed in this report.

As used in the above, "person acting on behalf of the Commission" includes any employee or contractor of the Commission, or employee of such contractor, to the extent that such employee or contractor of the Commission, or employee of such contractor prepares, disseminates, or provides access to, any information pursuant to his employment or contract with the Commission, or his employment with such contractor.

I. INTRODUCTION

In recent years several theoretical calculations have been made to predict the cross section for production of secondary particles in the interaction between high energy nucleons and complex nuclei.[1-9] These calculations are based on models which involve assumptions which cannot be fully justified theoretically; therefore, justification relies heavily on comparisons with experiment. There are numerous experiments, particularly for secondary protons and mesons, with which checks can be made;[10-14] however, little data exists above 200 MeV which systematically covers certain parameters such as atomic weight, angle, or energy. To provide data which systematically covers a range of elements, angles, and incident energies for comparison with the calculations, a series of experiments has been performed to investigate the secondary nucleon production in the interaction of primary protons bombarding complex nuclei.[15-17] The energy spectra of neutrons and protons presented here cover the region between 100 and 450 MeV from targets bombarded by 450 MeV protons and were measured for a number of elements ranging in atomic weight from beryllium to bismuth. Two categories of target thicknesses were studied: thin targets in which the primary beam lost little energy and the nuclear interaction mean free path is much larger than the target thickness, and thick targets in which the primary beam stopped or lost a large fraction of its energy and the target thickness was of the same order as the nuclear mean free path. The primary proton energy is well above the meson production threshold and data should be of particular value for comparison with calculations which include meson production and its effects on the nucleon production cross sections.

These measurements, made at the University of Chicago synchrocyclotron, are similar to those reported[17,18] for 160-MeV proton bombarding energy and the data was recorded and analyzed using a proton recoil spectrometer and analysis techniques similar to those employed in the 160-MeV measurements. In this paper, the experimental set-up will be described only briefly with emphasis on the modifications to the previous spectrometer and analysis techniques. For details of the methods used to analyze the data, the reader is referred to references 17 and 18.

II. EXPERIMENTAL SET-UP

The proton beam from the synchrocyclotron was focused with two quadrupole magnets to a spot size of approximately 3 cm^2 on the target, as shown in Fig. 1, and the spectrometer was placed at the appropriate angle behind the target. By using stochastic beam extraction, a duty cycle of approximately 25% was obtained.

The energy of the beam was measured using a range telescope with Cu absorbers. Using the tables of Barkas and Berger[19] and applying the multiple scattering correction of Janni,[20] the energy was found to be 450.4 ± 1 MeV. This corresponds to an effective range in Cu, including scintillators and light covers, of 144.0 gm/cm^2.

The incident proton beam was integrated with helium-filled ion chambers[21] calibrated using the $^{12}C(p,pn)$ reaction.[22] To accomplish this calibration a plastic scintillator larger than the beam spot was placed at the target position and exposed to the beam passing through the ion chambers. After exposure, the scintillator was placed on a photomultiplier tube and the activity induced by the C(p,pn) reaction was calculated

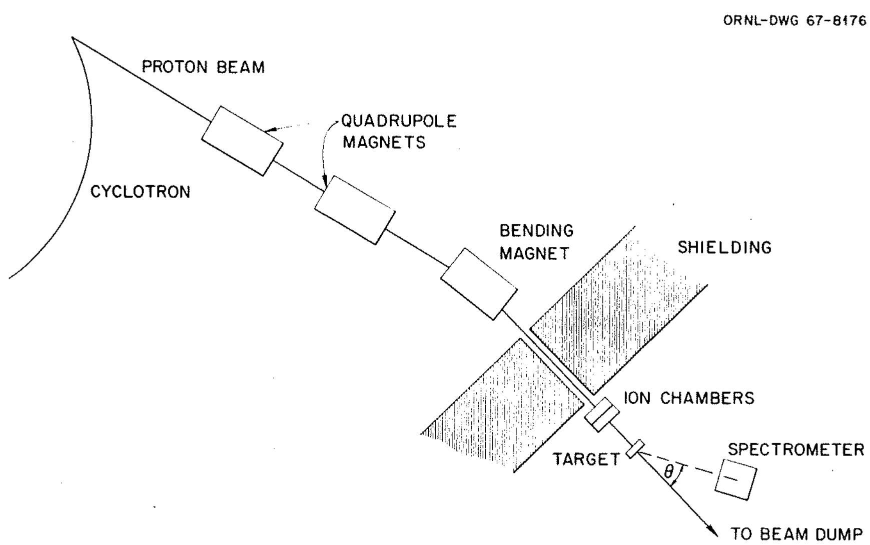

Fig. 1. Plan view of experimental set-up for measuring the neutron and proton spectra from targets bombarded by a 450-MeV proton beam.

from the positron counting rate. The cross section used for this calibration was 32.3 mb. A correction was made for the positrons with energies below the counting threshold. This calibration was compared with the value obtained by extrapolating a calibration obtained using a 160-MeV proton beam monitored with a Faraday cup, and the two values were found to agree to within 5%.

III. SPECTROMETER

The measurements were made using the proton recoil spectrometer shown in Fig. 2. The neutrons from the target impinged on the polyethylene radiator and the recoiling protons passed through the organic $\Delta E/\Delta X$ counter and produced pulses with a mean height

$$h \sim \int_0^T (d\ell/dE)(dE/dX)dX \ , \tag{1}$$

where $d\ell/dE$ is the scintillation efficiency and T is the thickness of the counter. Since for protons dE/dX and $d\ell/dE$ are monotonically decreasing functions of energy below approximately 2 BeV, the recoil proton energy may be determined from a measurement of pulse height. Fig. 3 is a plot of the pulse height from the $\Delta E/\Delta X$ counter as a function of the energy of the protons incident upon the scintillator. The relationship was obtained by exposing the $\Delta E/\Delta X$ counter to protons of various energies obtained by degrading the 450-MeV proton beam with copper absorbers. The energy E_p of the recoil proton is related to the energy E_n of the incident neutron by

$$E_p = E_n \cos^2 \theta/(1 + E_n \sin^2 \theta/2Mc^2) \ , \tag{2}$$

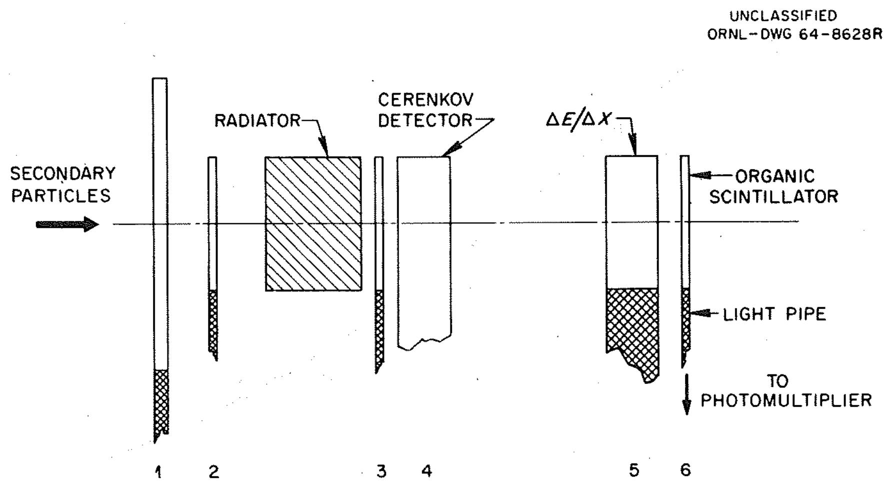

Fig. 2. Placement of counters and hydrogeneous radiator in proton recoil spectrometer.

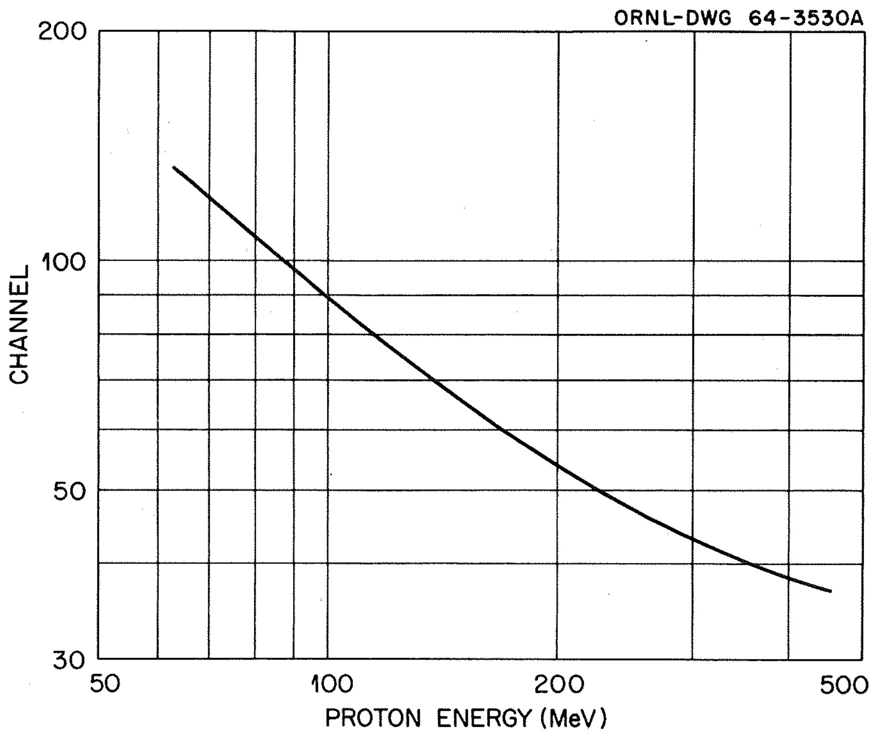

Fig. 3. Pulse height as a function of energy for protons traversing a 3.153-g/cm^2-thick plastic scintillator.

where θ is the angle between the path of the incident neutron and the recoil proton and M is the mass of a nucleon.

Counters 3 and 6 are placed in coincidence with the $\Delta E/\Delta X$ counter to reduce backgrounds from gamma rays and neutrons. Counter 6 also ensures that recoil protons which do not penetrate the $\Delta E/\Delta X$ counter are not counted.

The counters in front of the radiator were placed in anti-coincidence with the $\Delta E/\Delta X$ counter and served to reject counts due to protons present in the incident beam. In order to reduce the leak-through in the anti-coincidence channel due to the dead time caused by high random rates in the anti-coincidence counters, two counters were employed in a "neither/nor" configuration. Background measurements were made by replacing the polyethylene radiator with a carbon radiator containing the same amount of carbon as the polyethylene radiator. Proton spectra were measured by removing the radiator and the anti-coincidence requirements imposed by counters 1 and 2.

A severe background problem arose from mesons and high-energy electrons produced in the target, and, in the case of neutron measurements, in the radiator. Due to the large resolution of the spectrometer many of the pulses produced in the $\Delta E/\Delta X$ counter by these particles were of the same size as the pulses produced by the high-energy recoil protons. In the case of the neutron measurements, the production of these background counts was somewhat different in polyethylene radiator than in the carbon radiator and these effects could not be entirely eliminated by a background subtraction. In the case of proton measurements no background measurements were made for thick targets and the thin-target background measurements were made with the target out, resulting in an uncompensated residual background from the mesons and electrons. To reduce the number of these lighter particles which were counted, a Cerenkov counter with a threshold of $\beta = 0.67$ was placed in front of the $\Delta E/\Delta X$ counter and was connected in anti-coincidence. An event $\bar{1}\bar{2}3\bar{4}56$ was considered valid and a multi-channel analyzer was gated on and the pulse from the $\Delta E/\Delta X$ counter was stored.

The $\Delta E/\Delta X$ counter was a plastic scintillator[23] 3.0 cm-thick and 6.35 cm in diameter optically coupled to the photomultiplier tube with a light pipe glued to the cylindrical edge of the scintillator. The uniformity of light collection was improved by painting the scintillator with white paint[24] and was found to vary less than 5% over the volume of the scintillator.

IV. DATA ANALYSIS

Important considerations in the design of the spectrometer are the pulse height and energy resolution. The resolution of a distribution is defined as:

$$R = \frac{\text{full width at half maximum of distribution (FWHM)}}{\text{centroid of distribution}} .$$

The pulse-height resolution of the spectrometer for neutrons is that of the distribution obtained by exposing the spectrometer to a monoenergetic beam of neutrons. The important factors determining pulse height resolution are:

1. The range of scattering angles between the neutron and recoil protons.

2. The variety of energy losses in the radiator due to the various path lengths traveled by recoil protons.

3. Fluctuations of energy loss by the recoil protons in the $\Delta E/\Delta X$ scintillator.[25,26]

The energy resolution is defined as the resolution of the distribution obtained by transforming the above pulse-height distribution into an energy resolution using a one-to-one transformation between pulse height and energy. The contributions due to factors 1 and 2 can be readily controlled through the design of the spectrometer, and at the expense of efficiency can be reduced to small values. The contribution due to the third factor is determined by the thickness of the $\Delta E/\Delta X$ scintillator and decreases slowly with increasing scintillator thickness. For any reasonable choice of scintillator thickness the energy loss fluctuations for the higher energy protons were still large and were the determining factor on the practical resolution of the spectrometer. Due to the slow variation of dE/dX with proton energy at high proton energies the energy resolution was considerably larger. The spectrometer was designed so that the combined contributions from factors 1 and 2 were somewhat less than the maximum from 3.

The data were analyzed using the Simple Linear Optimization Procedure (SLOP)[27] code in the manner described previously.[17,18] Basically, the code is supplied with:

1. The raw pulse-height data.

2. The response functions of the spectrometer.

The response functions are the probability distributions that a particular energy particle will produce a pulse of a particular height.

Since it is not convenient to determine these distributions experimentally, they were calculated for the neutron measurements using a Monte Carlo code described previously[28] and combined with a calculation to incorporate the effect of energy loss fluctuations of the recoil protons in the $\Delta E/\Delta X$ scintillator. Typical results of this calculation are shown in Fig. 4. The total efficiency of the spectrometer for detecting neutrons was also calculated and the results for several different neutron energies are shown in Fig. 5. Proton spectra measurements were made by removing the radiator and anti-coincidence counters. In this case the response function is determined almost entirely by the energy loss fluctuations in the $\Delta E/\Delta X$ counter. However, in the case of the thin-target measurements in which the results are expressed as cross section, the distribution of energy losses of the secondary protons in the target is included in the response function so that the results are corrected to "zero-thickness targets." The pulse-height resolution of the spectrometer as a function of energy is given in Fig. 6 for protons.

The SLOP code calculates the range of energy spectra which is consistent with the raw data and the response functions. The energy response function associated with the output spectra is a Gaussian with a width specified by the user, and the results are presented in the form of a band which brackets the 68% confidence interval. The width of the confidence interval is determined jointly by the counting statistics, the error in determining the response functions, and the closeness of fit which is obtained between the desired Gaussian functions and a linear combination of the response functions.

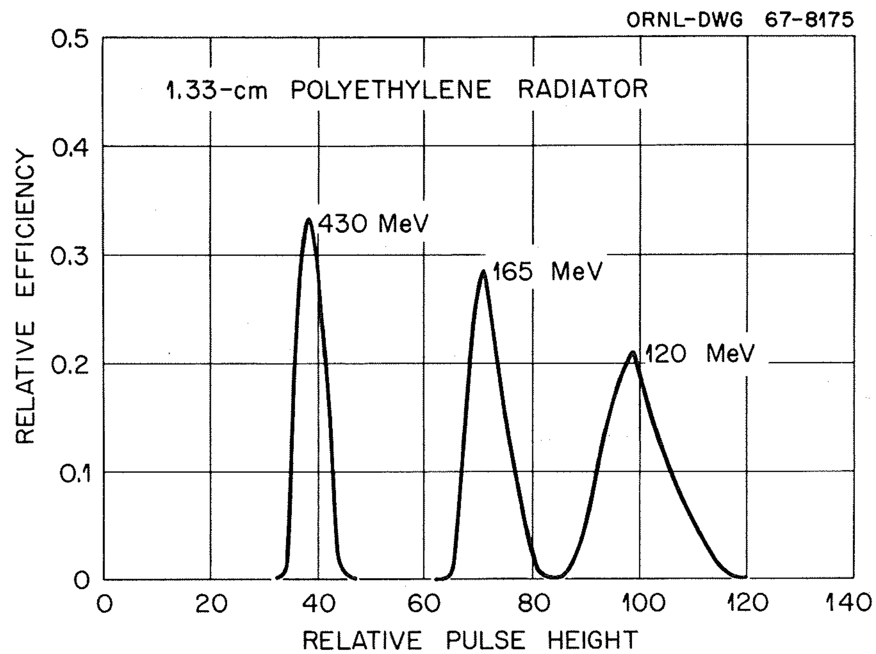

Fig. 4. Calculated pulse height distributions for monoenergetic neutron beams incident on the spectrometer with the 1.33 g/cm^2 radiator. The calculation was made using the Monte Carlo technique discussed in the text.

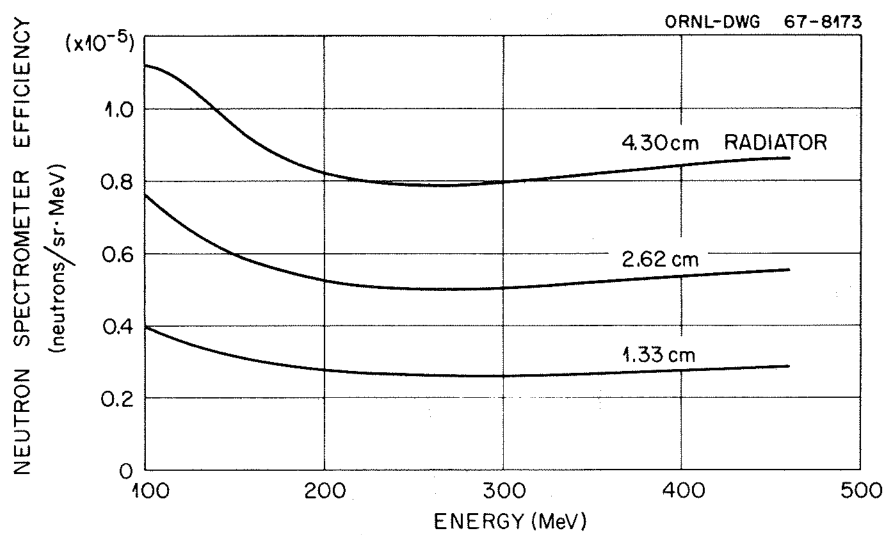

Fig. 5. Calculated neutron spectrometer efficiency for the polyethylene radiators used in the experiment. The calculation was made using the Monte Carlo technique discussed in the text.

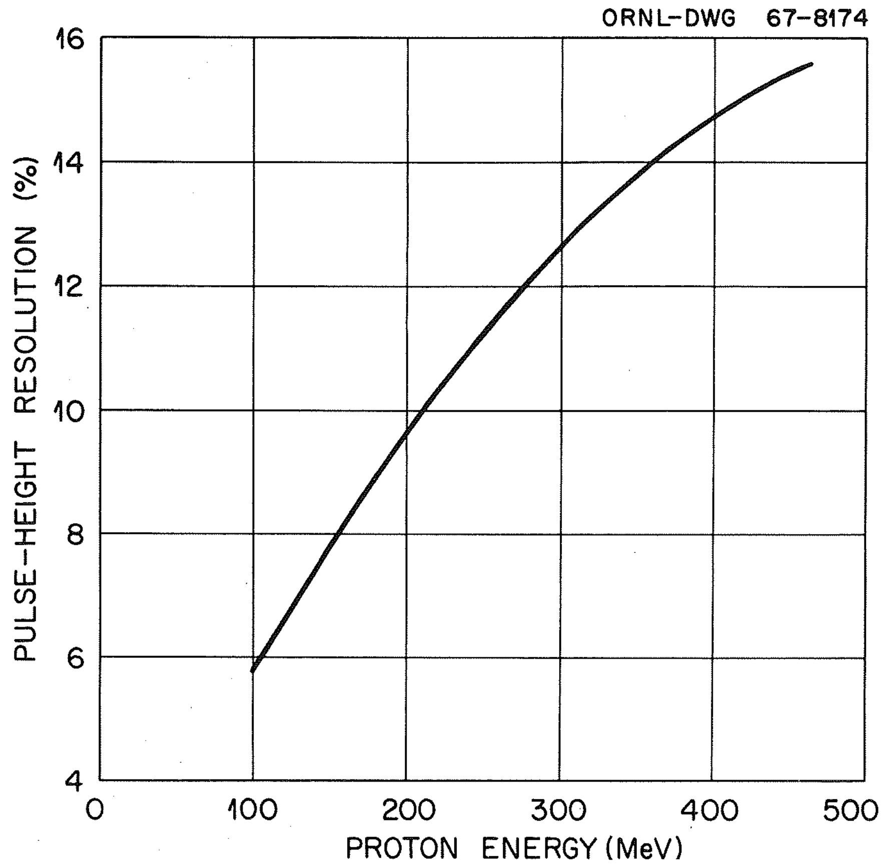

Fig. 6. Calculated pulse-height resolution as a function of energy for protons. In this case the major contribution to the resolution was the energy loss fluctuations in the $\Delta E/\Delta X$ counter and was the only effect included in these calculations.

V. RESULTS

Results from the neutron spectrometer measurements on both thick and thin targets are given in Figs. 7-14. These data were obtained using polyethylene radiators with thicknesses listed in Table I. Although in some measurements a 2.62-cm-thick radiator was used, most energy spectra were measured using both a 1.33- and a 4.30-cm-thick radiator and the results from these separate measurements combined in a statistically consistent manner to obtain the final energy spectrum. The energy resolution associated with these neutron energy spectra is Gaussian with a FWHM of 25%.

At high energies the effects of the gamma rays and meson leak-through were evident in the final spectra, and in the cases where the distortion was large the high-energy portion of the graph was omitted. In the cases where the distortion was small the graph was extrapolated into the distorted region as indicated by the dashed lines. At low energies the uncertainty in the spectra increased due to the large energy loss suffered by the recoil proton in the radiator and counters. The results were omitted in regions where the uncertainty was excessive.

Figure 7 shows the secondary neutron production cross section for a thin carbon target at laboratory angles of 20, 30, and 45°. These data show a broad peak in the cross section which appears at about 320 MeV for the 20° data, and at lower energies and increasingly less pronounced at greater angles of observation. This peak is seen also in the 6.73 g/cm^2 aluminum shown in Fig. 8, although the peak is less well defined at either 20° or at 30°. Similarly, the results from the 7.68 g/cm^2 cobalt target also show this peak.

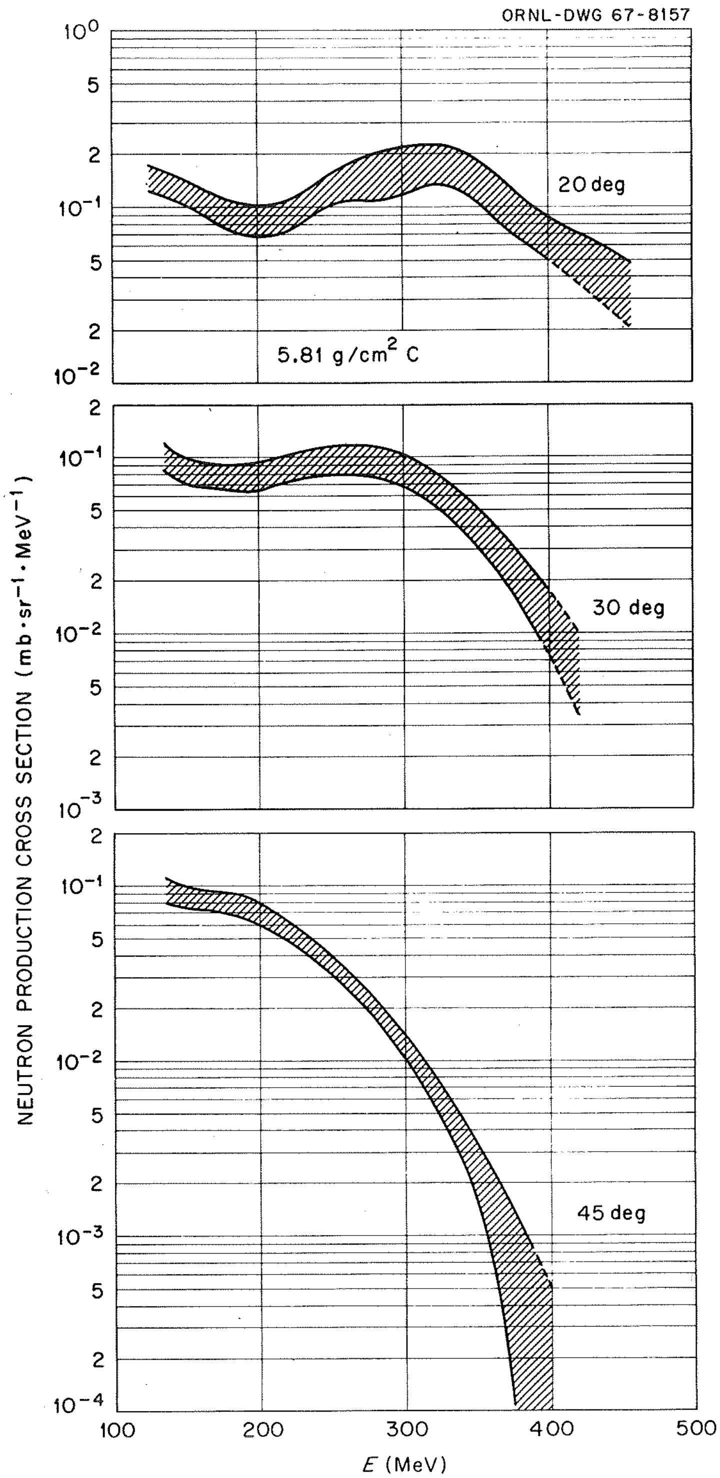

Fig. 7. Secondary neutron production cross section at 20, 30, and 45° for carbon bombarded by 450 MeV. The energy resolution associated with the spectra is Gaussian with a FWHM of 25%. The lines enclose the 68% confidence interval and include statistical uncertainties, uncertainties in calculating the efficiency of the spectrometer and the degree to which the computer program is not able to fit the spectrometer response functions with the Gaussian energy resolution functions.

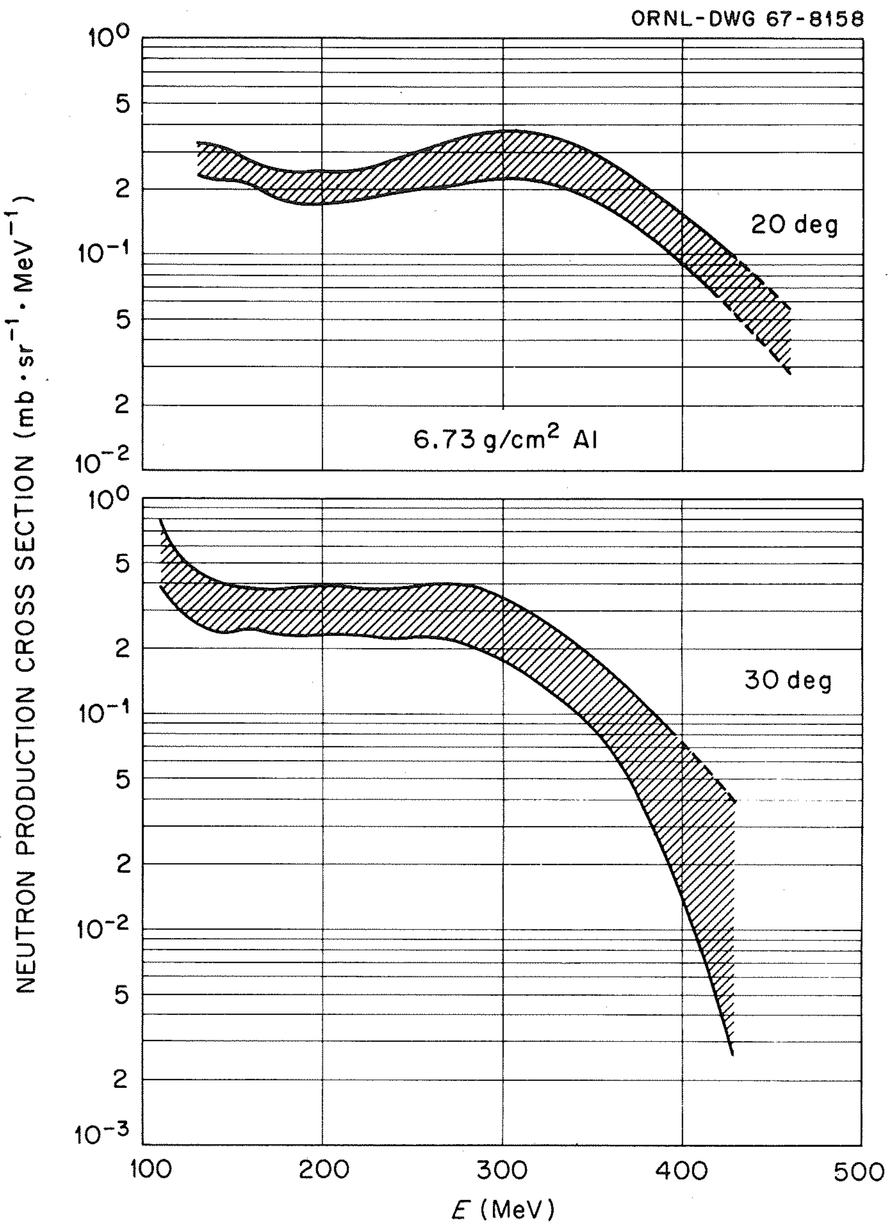

Fig. 8. Secondary neutron production cross section at 20 and 30° for a 6.73 g/cm² aluminum target.

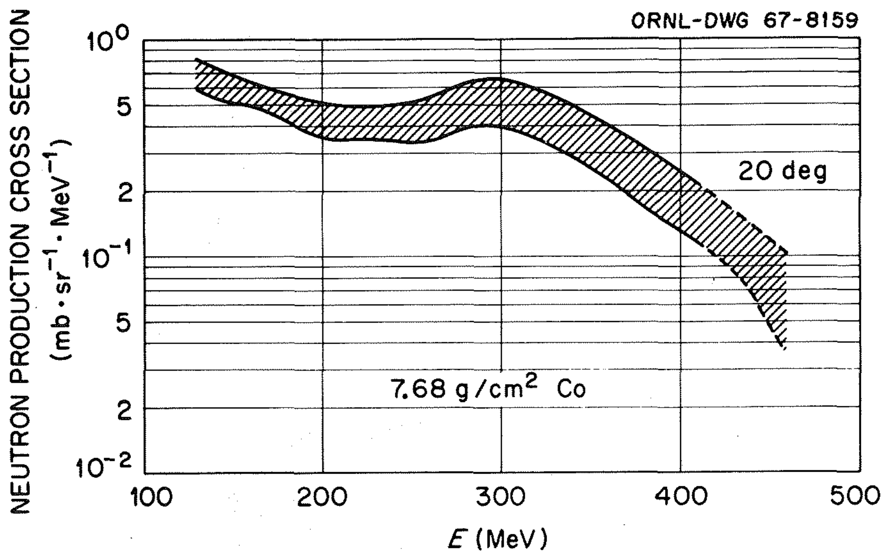

Fig. 9. Secondary neutron production cross section at 20° for a 7.68 g/cm² cobalt target.

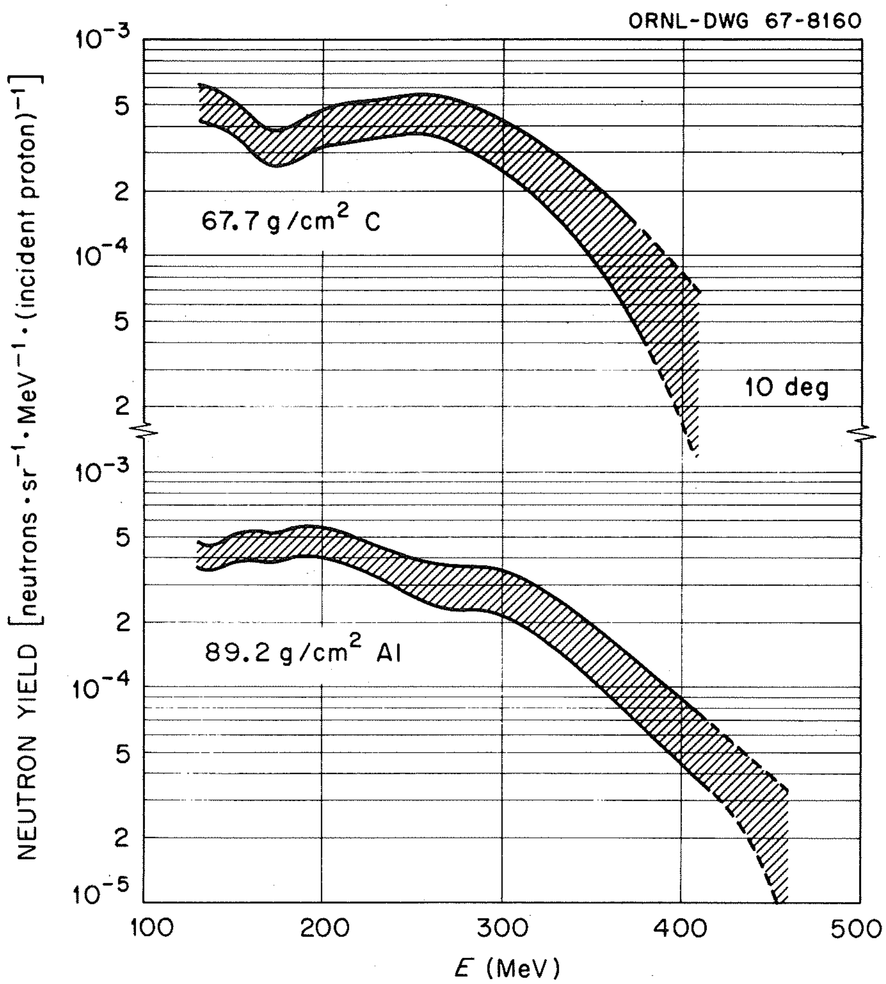

Fig. 10. Secondary neutron yield spectra at 10° to a 67.7 g/cm² carbon and a 89.2 g/cm² aluminum target.

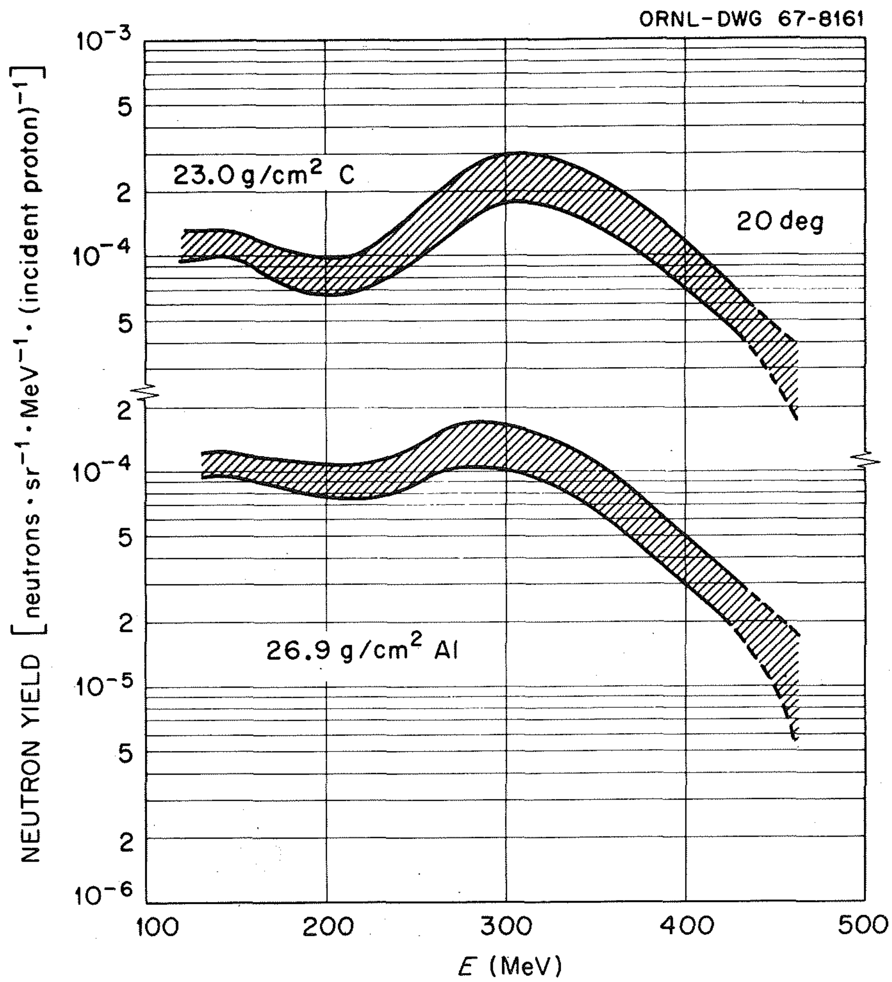

Fig. 11. Secondary neutron yield spectra at 20° to a 23.0 g/cm² aluminum target.

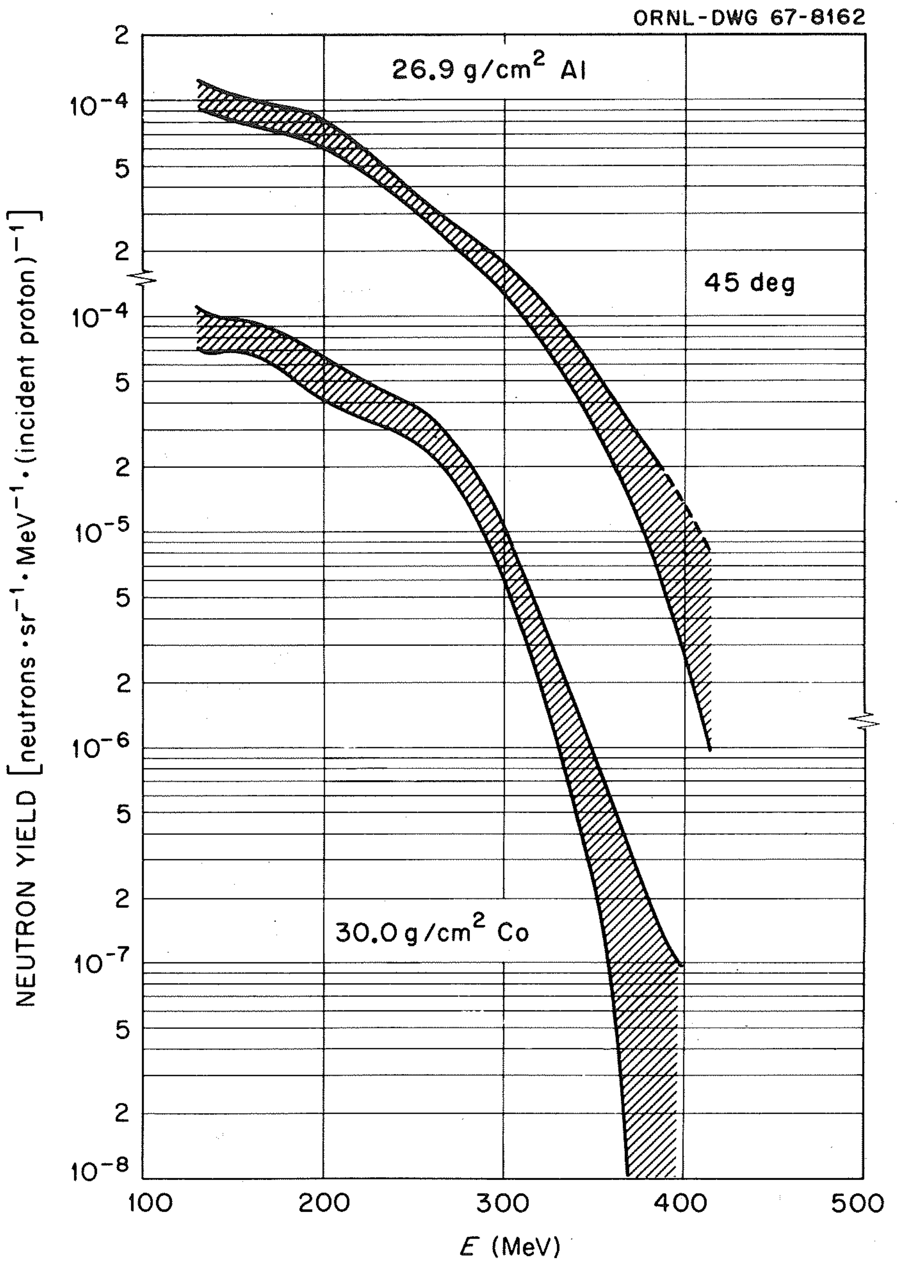

Fig. 12. Secondary neutron yield spectra at 45° to a 26.9 g/cm^2 aluminum and a 30.0 g/cm^2 cobalt target.

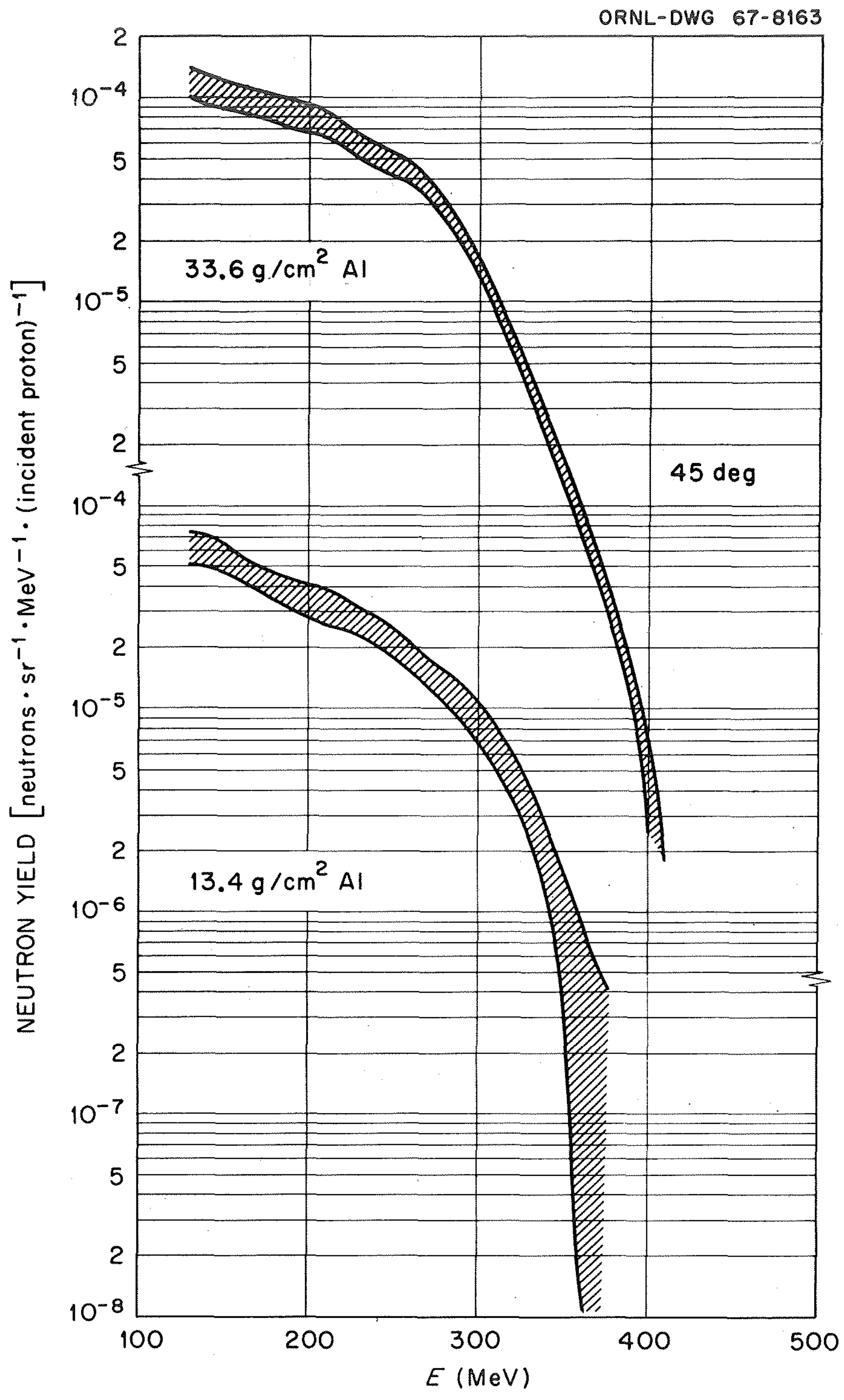

Fig. 13. Secondary neutron yield spectra at 45° to a 33.6 g/cm² and a 13.4 g/cm aluminum target.

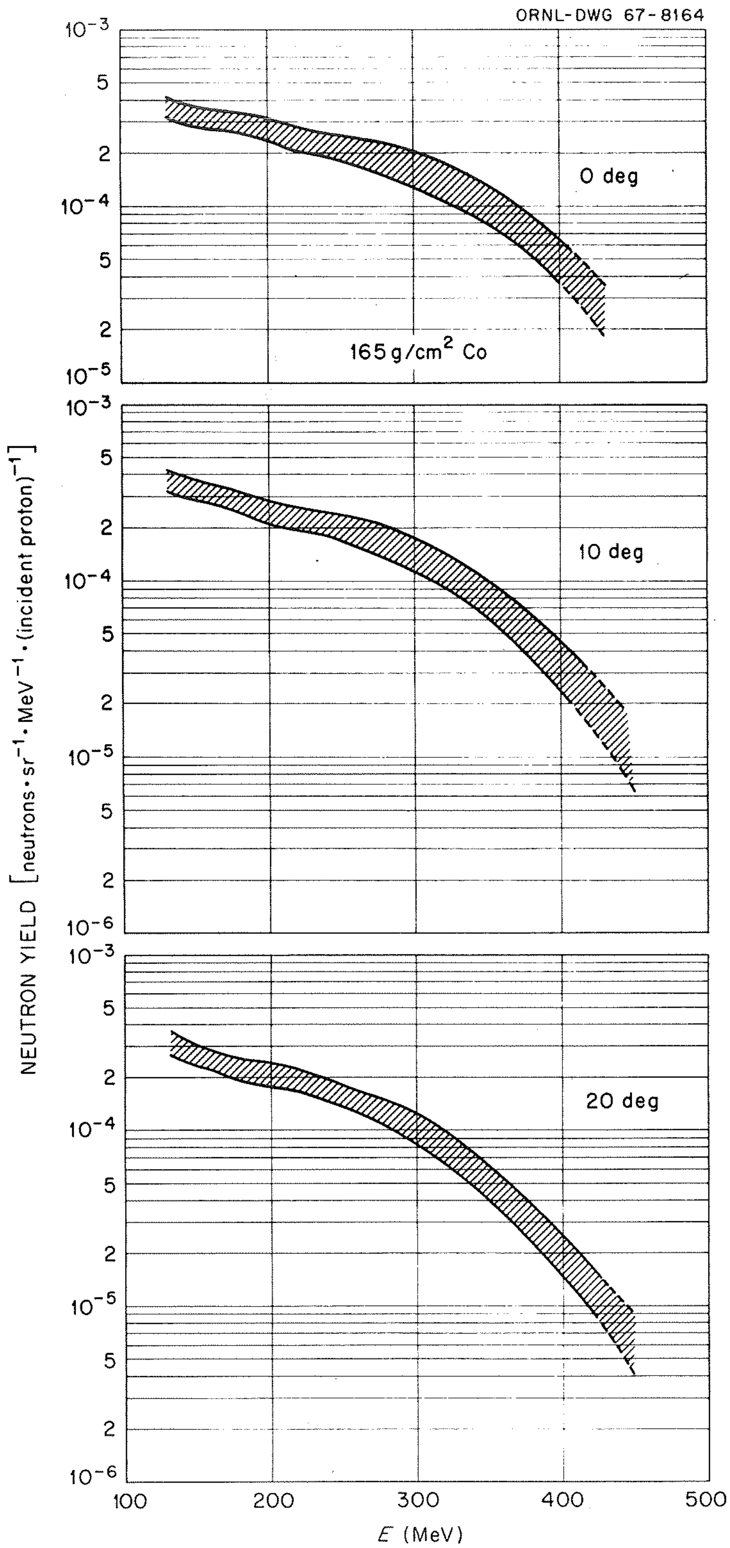

Fig. 14. Secondary neutron yield spectra at 0, 10, and 20° to a 165 g/cm² cobalt target.

Table I

Radiator Thickness (cm)	Energy of proton which loses 10% of its energy in radiator
1.33	100
2.62	150
4.30	200

This peak can be identified as due to the "quasi-elastic" scattering process, and is characteristic of both the neutron and proton spectra taken at angles below 45°. It is attributed to a process in which the incident particle interacts directly with an individual nucleon within the target nucleus and the product nucleon emerges with essentially the same energy and at the same angle as for an interaction between free nucleons. For light nuclei, the probability is high that the emerging nucleon does not undergo a further interaction with other target nuclei, and the peak is clearly defined. For heavy nuclei, these particles interact with other nucleons and the peak is characteristically broadened and shifted downward in energy as seen in Figs. 8 and 9.

Thick-target secondary neutron data are presented in Figs. 10-14. In these measurements, the laboratory angle was measured between the incident beam axis and the spectrometer axis at their point of intersection in the rear face of the target. The yield for all neutron energies was based upon the calculation of spectrometer efficiency assuming all particles were formed at the center of the target. The distance from the center of the radiator to this point is given in Table II for each of the measurements.

Figure 10 shows the secondary neutron energy spectra for a 67.7 g/cm^2 carbon target and an 89.2 g/cm^2 aluminum target at an angle of observation of 10°. The primary protons lost approximately 200 and 240 MeV, respectively, in passing through these targets.

Figures 11 and 12 show neutron yield spectra at 20 and 45° for targets in which a normally incident proton beam would lose approximately

Table II. Parameters of Neutron Measurements

Element	Thickness (g/cm²)	Angle[a] (deg)	Distance to Center[b] of target (cm)
		Cross Sections	
carbon	5.81	20	57.8
carbon	5.81	30	57.7
carbon	5.81	45	57.4
aluminum	6.73	20	57.4
aluminum	6.73	30	45.2
cobalt	7.68	20	56.7
		Yields	
carbon	67.7	10	75.7
carbon	23.0	20	62.5
aluminum	89.2	10	72.7
aluminum	33.6	45	60.1
aluminum	26.9	20	61.0
aluminum	26.9	45	59.9
aluminum	13.4	45	57.2
cobalt	165	0	66.1
cobalt	165	10	66.0
cobalt	165	20	65.6
cobalt	30.0	45	58.0

[a]The angles are measured between the primary proton beam line and the spectrometer axis. The targets were inclined so that a perpendicular to the target plane made an angle of 15, 22.5 and 30 deg to the beam axis for the spectrometer angles of 30, 45, and 60 deg, respectively. The beam, target and spectrometer axes lay in the same plane.

[b]This distance is measured from the center of the target to the effective center of the radiators.

60 MeV. In Fig. 13, the yields at 45° for aluminum targets of 33.6 and 13.4 g/cm^2 are compared.

In contrast to the "thin" targets, the larger energy loss of the incident proton beam within the target means that the observed particles include both secondary particles from interactions with incident protons of a wide range in energies and also tertiary particles.

Secondary neutron production from a 165 g/cm^2 cobalt target is shown in Fig. 14 for angles of 0, 10, and 20°. This target thickness is about 14% greater than the mean range of the incident proton beam.

Measurements of secondary proton production were made by removing the radiator and anti-coincidence counters from the spectrometer. Proton cross-section measurements utilized targets in which the primary proton beam lost 6.7 MeV in traversing the target at normal incidence (see Table III). The calculated response functions took account of the energy loss of the secondary protons in the targets to produce cross sections corrected to "zero target thickness." The energy resolution associated with the spectra is Gaussian with a FWHM of 20%.

Figures 15-17 show secondary proton production cross sections at angles of 30, 45, and 60° for various targets. For angles greater than 30° the target was turned through an angle of one-half the angle of observation about an axis passing through the same point. The quasi-elastic peak seen in the 30° cross-section data decreases in mean energy with increasing angle of observation and broadens with nuclear size.

Figures 18-21 compare proton yields for several angles of observation from thick targets of C, Cu, Pb, Al, and Co. Since the low-energy secondary protons lost considerable energy in escaping the target, no

Table III. Parameters of Proton Measurements[a]

Element	Thickness (g/cm^2)	Angles[b] (deg)
	Cross Sections	
beryllium	2.65	30,45,60
carbon	2.48	30,45,60
aluminum	2.80	30,45,60
cobalt	3.22	30,45,60
bismuth	4.50	30,45,60
	Yields	
carbon	5.81	20,30,45
aluminum	6.73	20
copper	5.65	30,45,60
cobalt	165	0
cobalt	7.68	20
lead	3.60	30,45,60

[a]The distance from the back counter of the spectrometer to the center of the back face of the target was 74.82 cm.

[b]This distance is measured from the center of the target to the effective center of the radiators.

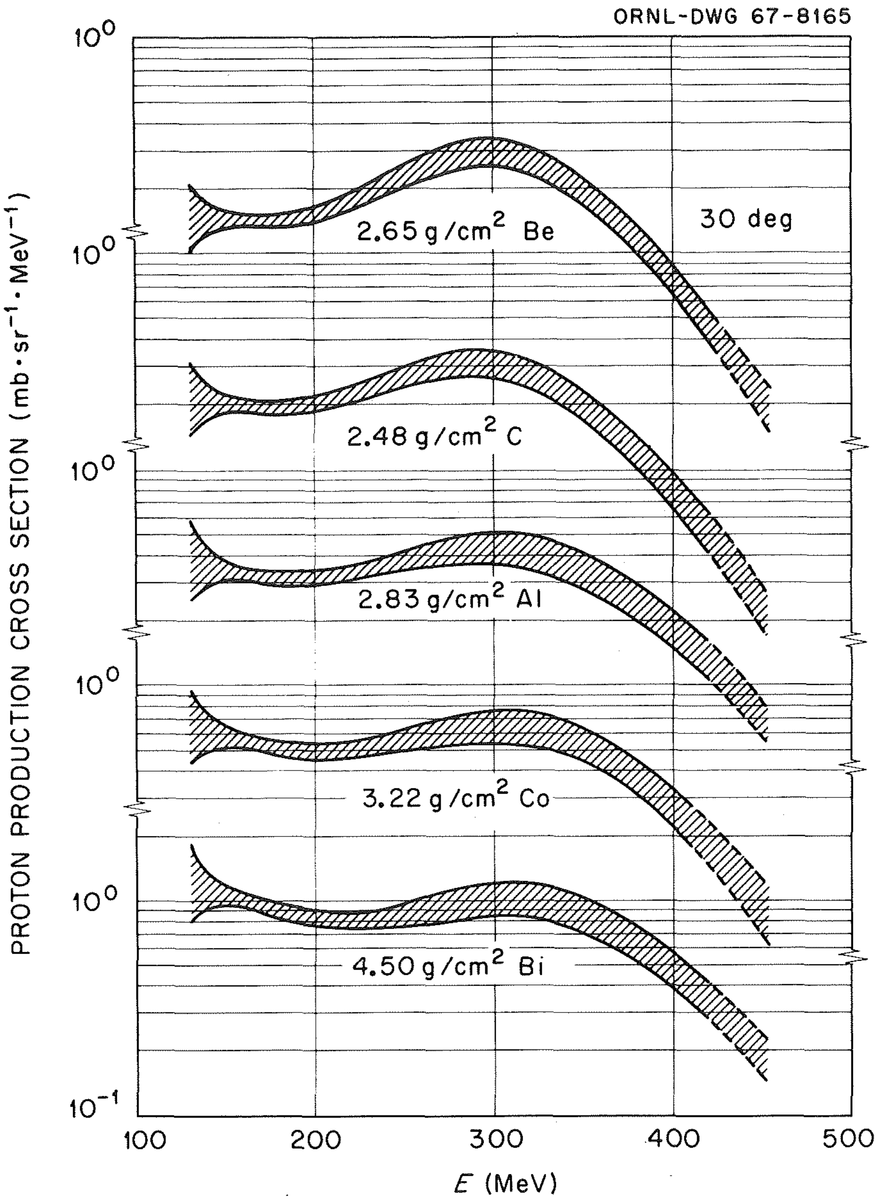

Fig. 15. Secondary proton production cross sections at 30° for various targets bombarded by 450-MeV protons.

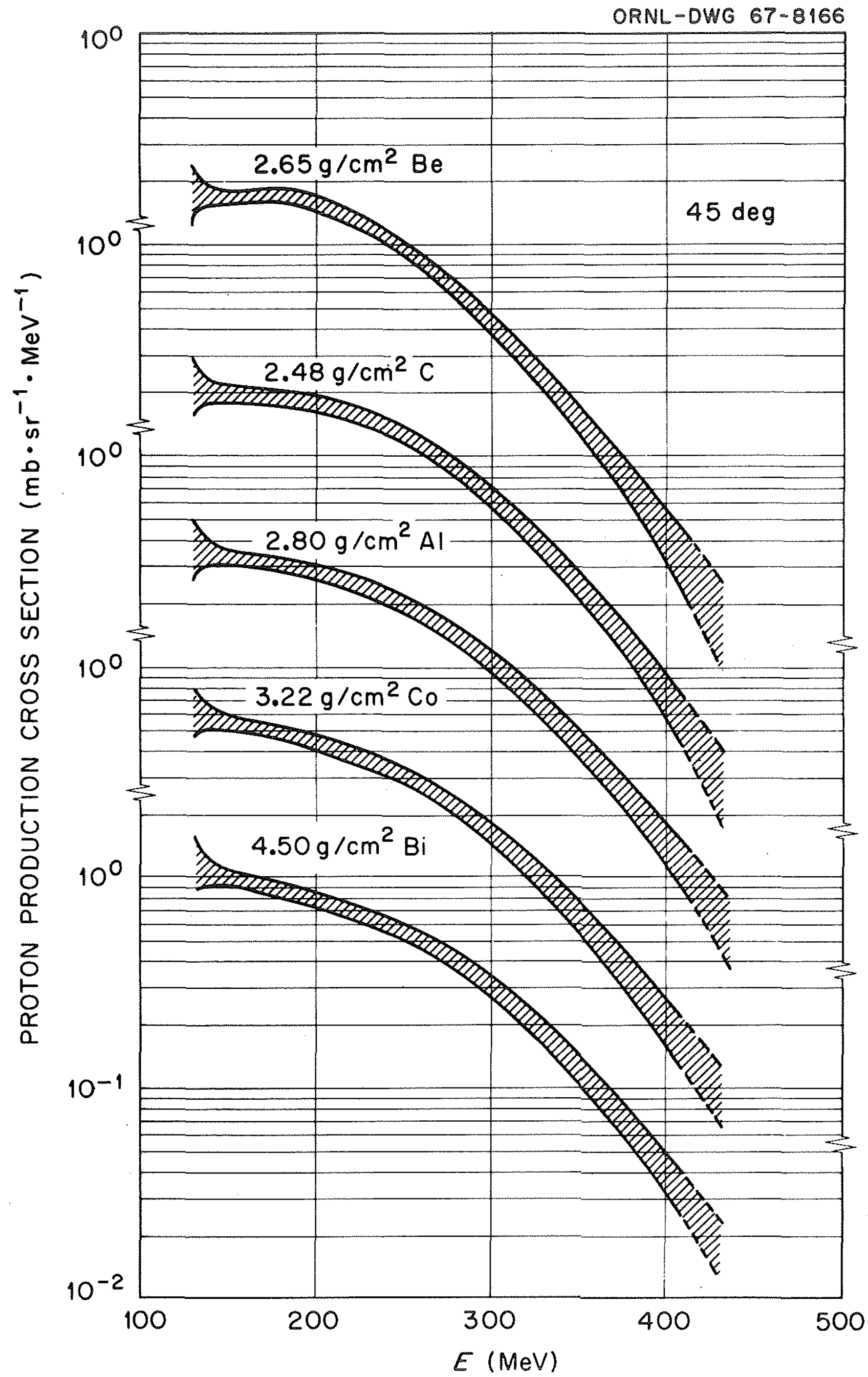

Fig. 16. Secondary proton production cross sections at 45 for various targets bombarded by 450-MeV protons.

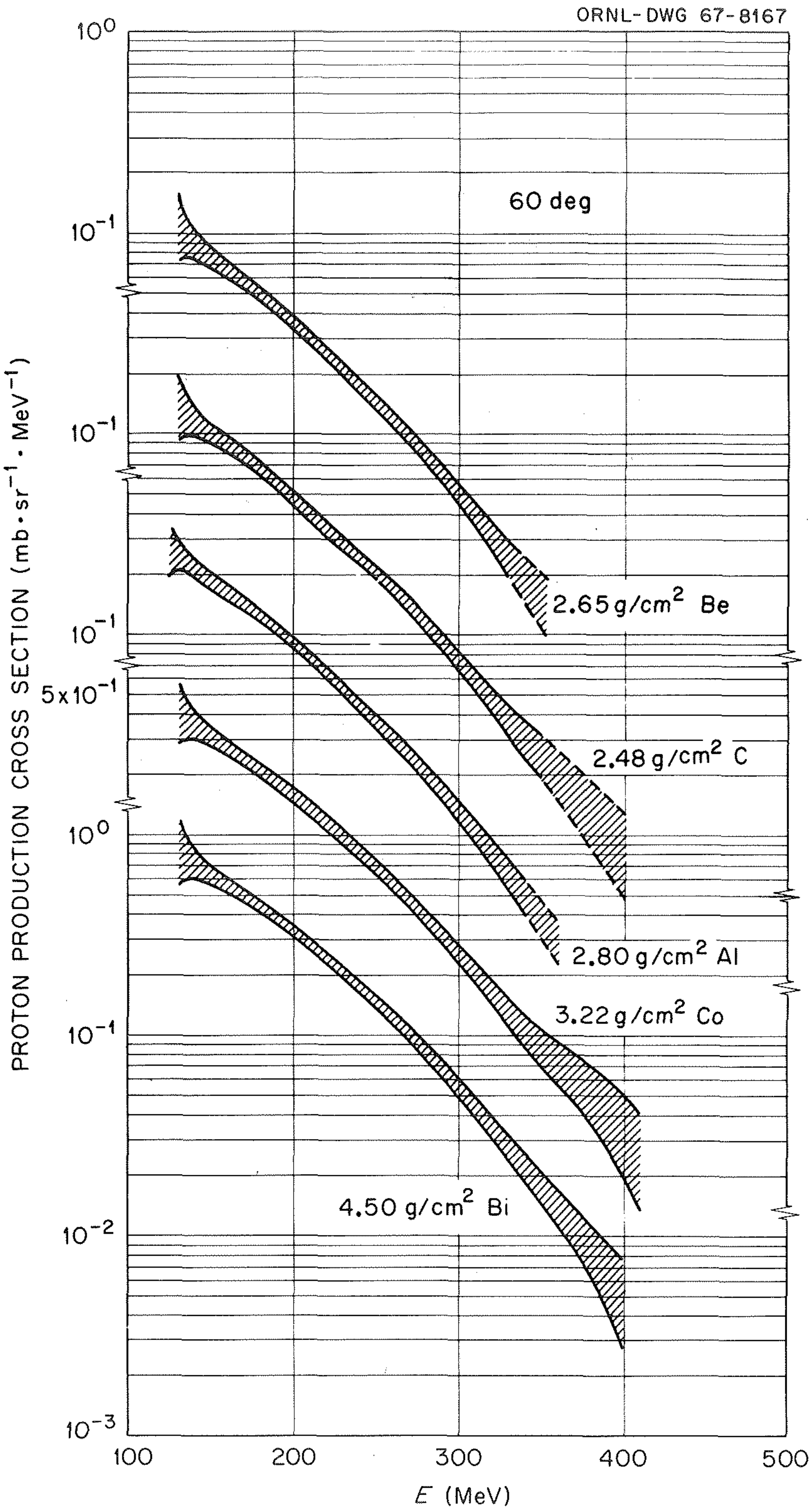

Fig. 17. Secondary proton production cross sections at 60° for various targets bombarded by 450-MeV protons.

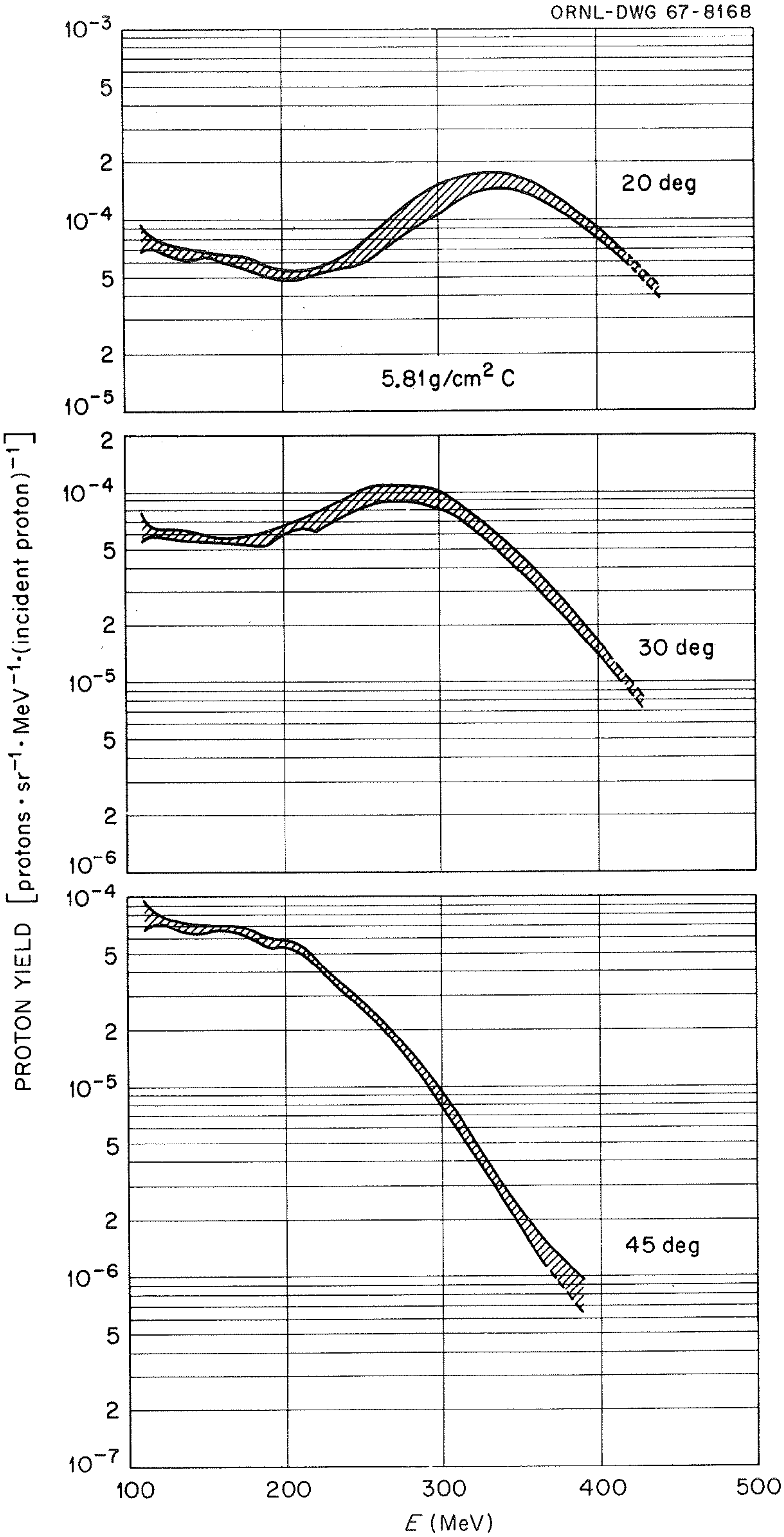

Fig. 18. Secondary proton yield at 20, 30, and 45° from a 5.81 g/cm² carbon target.

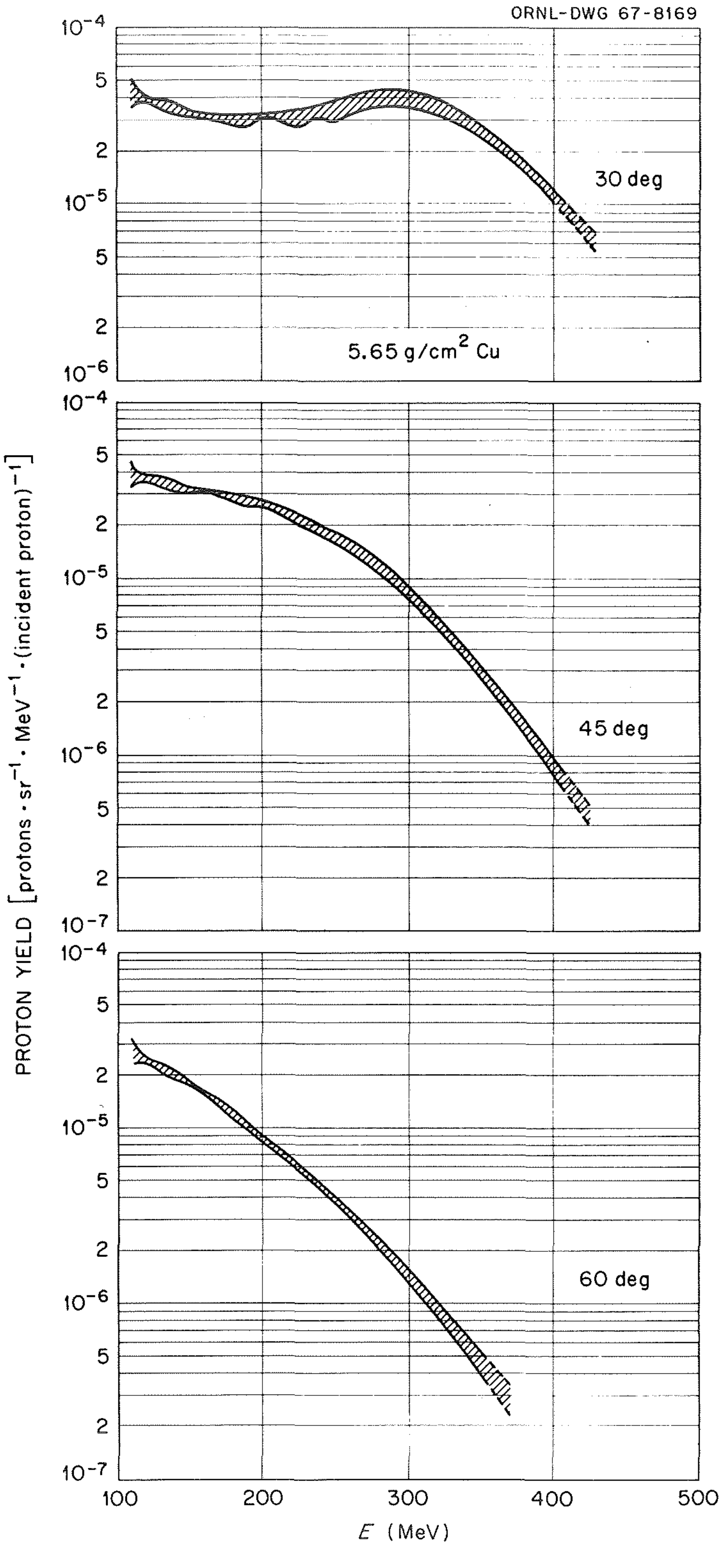

Fig. 19. Secondary proton yield at 30, 45, and 60° from a 5.65 g/cm² copper target.

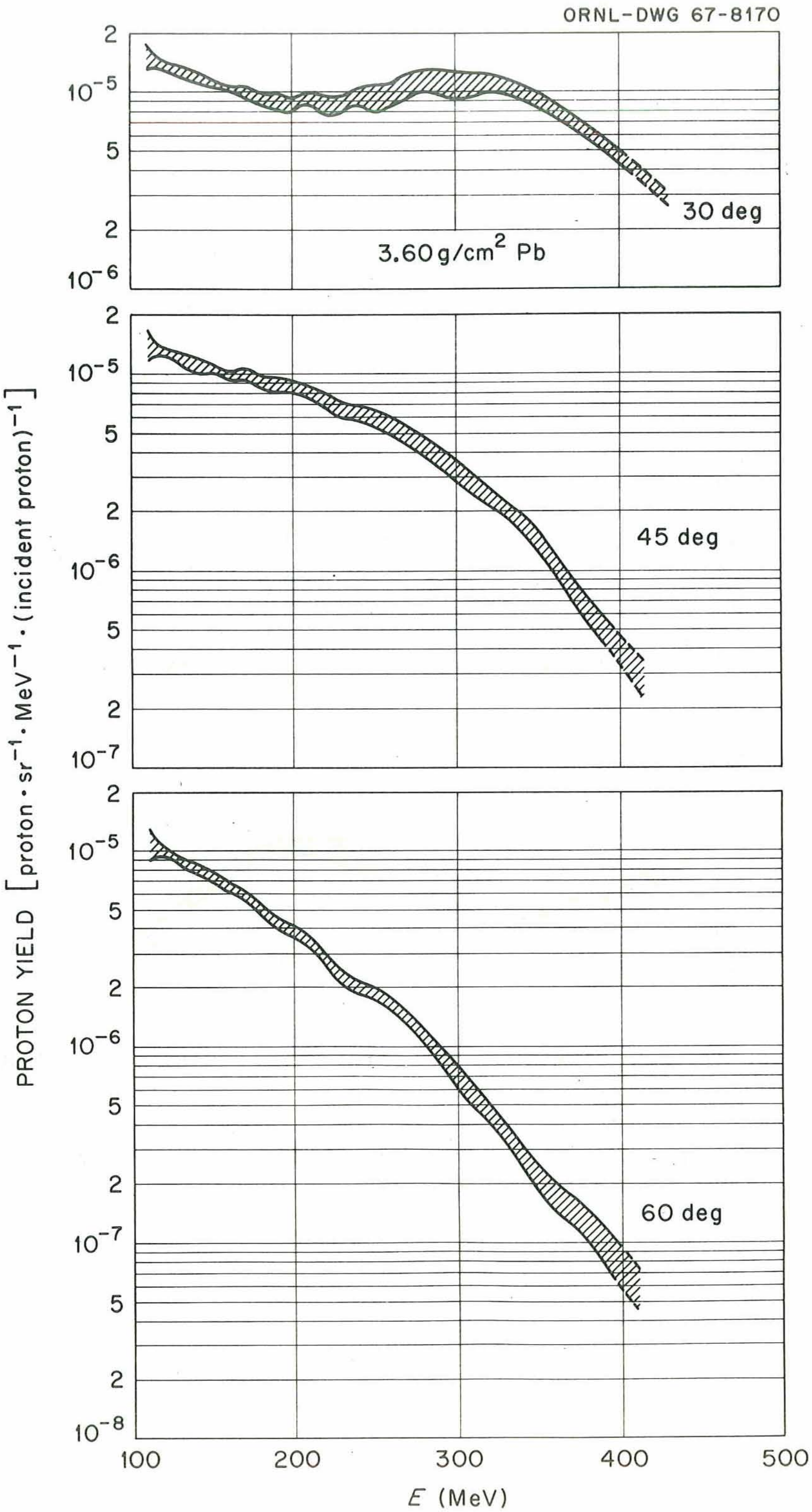

Fig. 20. Secondary proton yield at 30, 45, and 60° from a 3.20 g/cm² lead target.

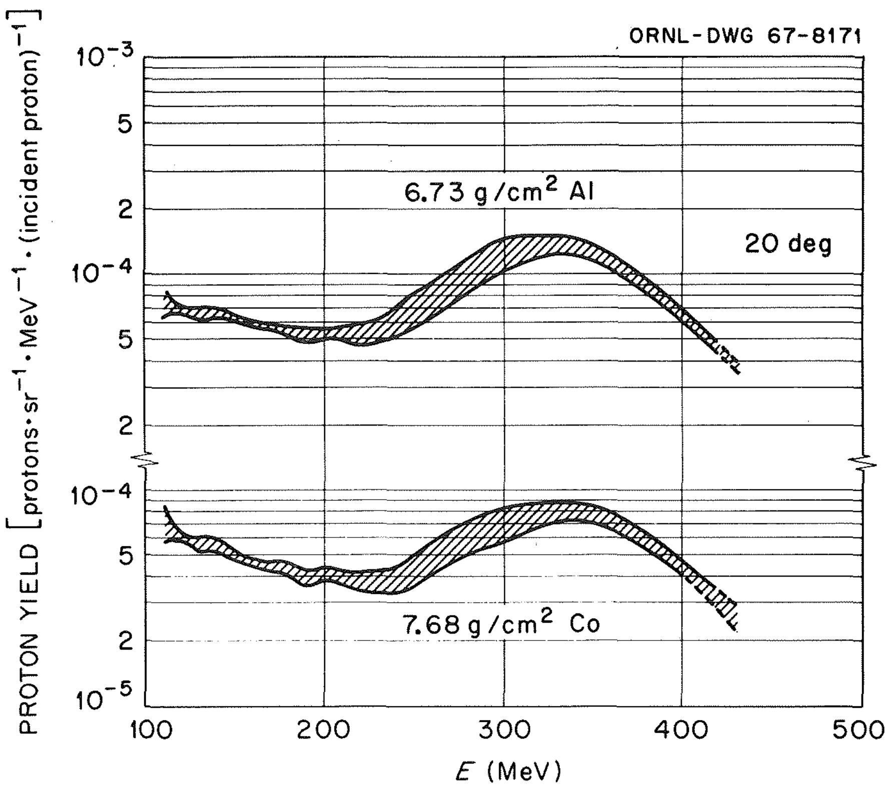

Fig. 21. Secondary proton yield at 30, 45, and 60° from a 6.73 g/cm^2 aluminum and a 7.68 g/cm^2 cobalt target.

attempt was made to include this loss in the response functions and the spectra represent the energy of the protons as they leave the rear face of the targets. Although the 3.6 g/cm^2 Pb target was "thin," it had a non-standard thickness and, therefore, the data from this target is presented as a yield.

Figure 22 shows the proton yield at 0^o from a 165 g/cm^2 cobalt target. Since the primary proton beam was completely stopped in this target, the observed yield is due to tertiary protons.

In those data in which there is evidence for a quasi-elastic peak, the energy of the peak is lower than would be expected on the basis of a simple nucleon-nucleon interpretation. The nuclear cascade description of high-energy interactions as typified by the Monte Carlo calculations of Bertini[5] would indicate that at lower energies and for 0^o measurements the emerging nucleon, whether proton or neutron, can have essentially the energy of the incident proton. The peak as a function of angle should appear at energies given approximately by

$$T = \frac{E_o \cos^2\theta}{(1 + E_o \sin^2\theta/2mc^2)} - V_o \qquad (3)$$

where θ = the angle of observation, m = the mass of the nucleon, V_o = the average nuclear potential of the bound nucleons, $E_o = T_o + V_o$, and T and T_o = kinetic energy of emerging particle and the incident particles, respectively. Data at higher energies for Be targets[39] show that the neutron peak at 0^o also appears at a lower energy: 680-MeV protons produce a neutron peak at 610 MeV and 480-MeV protons show a neutron peak at 395 MeV. The internal beam of the cyclotron was used for these measurements so that multiple traversal of the target by the bombarding protons was

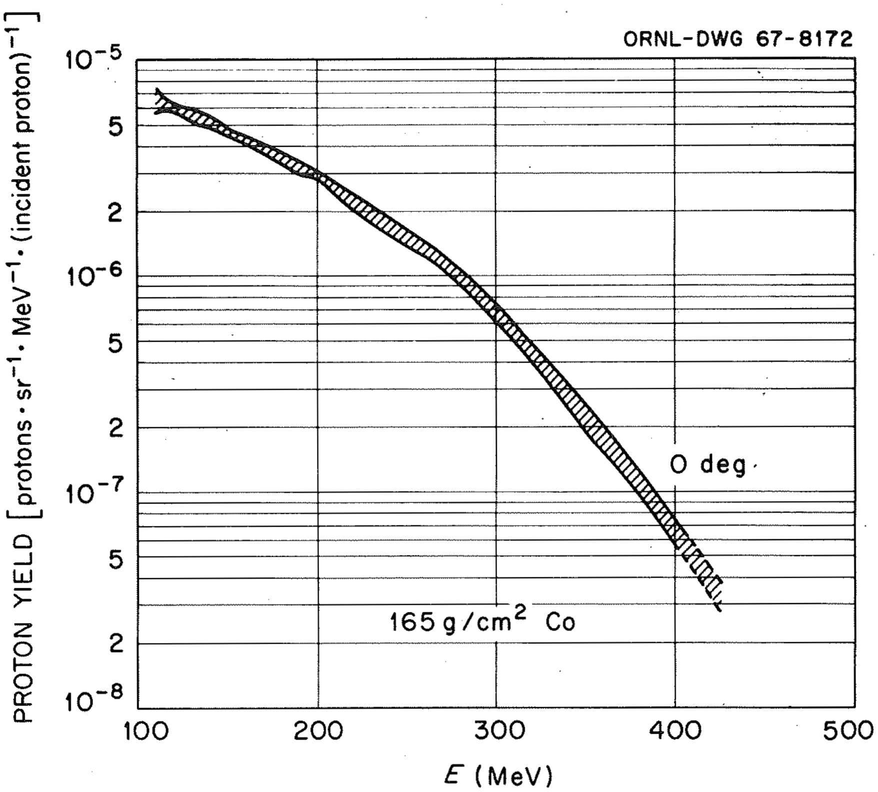

Fig. 22. Proton yield at 0 from a 165 g/cm² cobalt target. The primary proton beam was completely stopped in this target.

possible. The magnitude of the consequent energy reduction has been estimated by Kiselev and Fliagin[30] as 20 to 25 MeV. These data, therefore, indicate a net shift to lower energies of 55-60 MeV. Such a reduction in the neutron energy at 0° is consistent with the mean peak energy reduction seen in the data reported here.

Multiple scattering and cascading not only considerably broaden the peak but also lower its mean energy. Secondary meson production also causes a reduction in the peak energy, particularly at the higher bombarding energies. Indeed, preliminary calculations, using Bertini's Monte Carlo programs in which secondary meson production was or was not included, indicate that meason production must be taken into account in order to obtain correlation with the observed spectra.[31]

These data cover a wide range of atomic number and angles and provide information to make detailed comparisons with stochastic calculations. Comparisons of these data with the calculations cited above show qualitative agreement with theory.

VI. ACKNOWLEDGMENTS

The authors wish to thank the Physics Department of the University of Chicago and the Department of the Navy for making the machine available. The help of the synchrocyclotron staff is also appreciated. The aid of N. W. Hill of the Oak Ridge National Laboratory in the design of electronics and in the performance of the experiment is gratefully acknowledged.

REFERENCES

[1]M. L. Goldberger, Phys. Rev. 74, 1269 (1948).

[2]N. Metropolis et al., Phys. Rev. 110, 185 (1958).

[3]U. S. Barashenkov et al., Nucl. Phys. 14, 522 (1959/60).

[4]E. Abate et al., Nuovo Cimento 22, 1206 (1961).

[5]H. W. Bertini, Phys. Rev. 131, 1801 (1963); Phys. Rev. AB2(1965).

[6]K. Chen et al., Intern. Conf. on Interactions of High Energy Particles with Complex Nuclei, Leysin (1963).

[7]E. Gradsztajn, J. Phys. Radium 24, 829 (1963).

[8]A. Avni et al., Monte Carlo Program for the Interactions of High Energy Particles with Complex Nuclei, Leysin (1963).

[9]J. P. Cohen, Nucl. Phys. 84, 316 (1966).

[10]K. Strauch and F. Titus, Phys. Rev. 104, 191 (1956).

[11]J. M. Cassels, T. C. Randle, T. G. Pickavance, and A. E. Taylor, Phil. Mag. 42, 215 (1951).

[12]J. B. Cladis, W. N. Hess, and B. J. Moyer, Phys. Rev. 87, 425 (1952).

[13]A. G. Meshkovskii, Iu. S. Pligin, Ia. Ia. Shalamov, and V. A. Shebanov, JETP 4, 842 (1957).

[14]L. S. Azhgirey et al., Nucl. Phys. 13, 258 (1959).

[15]R. W. Peelle, T. A. Love, N. W. Hill, and R. T. Santoro, Phys. Rev. 167, 981 (1968).

[16]W. Zobel, F. C. Maienschein, and R. J. Scroggs, Spectra of Gamma Rays Produced by the Interaction of ~160 MeV Protons with Be, C, O, Al, Co, and Bi, ORNL-3506 (1965).

[17]J. W. Wachter, W. R. Burrus, and W. A. Gibson, Phys. Rev. 161, 971 (1967).

[18]W. A. Gibson, W. R. Burrus, J. W. Wachter, and C. F. Johnson, Nucl. Instr. and Methods 46, 29 (1966).

[19]W. Barkas and M. Berger, National Academy of Sciences-National Research Council, Publication No. 1133, p. 103 (1964).

[20]J. F. Janni, Calculation of Energy Loss, Range, Path Length, Straggling, Multiple Scattering, and the Probability of Inelastic Nuclear Collisions for 0.1 to 1000 MeV Protons, Technical Report No. AFWL-TR-65-150 (September 1966).

[21]R. T. Santoro and R. W. Peelle, Measurement of the Intensity of the Proton Beam of the Harvard University Synchrocyclotron for Energy-Spectral Measurements of Nuclear Secondaries, ORNL-3505 (1964).

[22]J. B. Cumming, Ann. Rev. of Nucl. Sci., Vol. 13, p. 261. Annual Review, Inc., California (1964).

[23]NE-102 manufactured by Nuclear Enterprises, Winnipeg, Canada.

[24]Water-base reflector paint manufactured by Nuclear Enterprises, Winnipeg, Canada.

[25]B. Rossi, High Energy Particles, Ch. 2, p. 22, Prentice Hall, New York (1952).

[26]D. M. Ritson, "General Properties of Particles and Radiation," Techniques of High Energy Physics, edited by D. M. Ritson, Interscience Publishers, Inc., New York (1961).

[27]W. R. Burrus and V. V. Verbinski, American Nuclear Society Report No. ANS-SD-2 (1965).

[28]W. E. Kinney and J. W. Wachter, Neutron Physics Division Annual Progress Report for Period Ending August 1, 1963, ORNL-3499 (1963).

[29] V. P. Dzhelepov *et al.*, Izv. Akad. Nauk SSSR Ser. Fiz. *19*, 573 (1955).

[30] V. Kiselev and V. B. Fliagin, JETP *32*, 962 (1957).

[31] H. W. Bertini and J. W. Wachter, *Neutron Phys. Div. Ann. Progr. Rept.*, May 31, 1968, paper 6.5,ORNL-4280.

NASA-High Energy Distribution List

R. M. Ahrens, Advanced Research Corporation, 715 Miami Circle, N.E., Atlanta, Georgia 30324

Donald W. Aitken, Research Physicist, Stanford University, Department of Physics, Stanford, California

Argonne National Laboratory, Library Services Department 203-CE125, 9700 South Cass Avenue, Argonne, Illinois 60439

Army Materials and Mechanics Research Center, ATTN: Technical Information Branch, Watertown, Massachusetts 02172

Louis Avrami, Radiation Effects and Support Branch, Explosives Laboratory, SMUPA-VE3, Bldg. 407, Picatinny Arsenal, Dover, New Jersey 07801

Miguel Awschalom, National Accelerator Laboratory, P. O. Box 500, Batavia, Illinois 60510

M. Barbier, CERN, Geneva, Switzerland

N. Barr, Radiological Physics Branch, Division of Biology and Medicine, U. S. Atomic Energy Commission, Washington, D. C. 20545 (5 copies)

C. K. Bauer, Dept. 72-34, Z-26, Lockheed-Georgia Company, Marietta, Georgia 30060

Sherwin M. Beck, NASA/Langley Research Center, Mail Stop 400, Hampton, Virginia 23365

P. R. Bell, Code TH, NASA/Manned Spacecraft Center, Houston, Texas 77058

J. R. Beyster, 9321 LaJolla Farms Road, LaJolla, California 92112

Frank L. Bouquet, Dept. 72-71, 311, B-6, Lockheed California Co., Burbank, California 91503

S. Bristicker, Grumman Aircraft Engineering Corp., Space Sciences Group, Plant 5, Bethpage, L. I., New York 11714

Charles J. Bridgman, Physics Department, School of Engineering, Air Force Institute of Technology, Wright-Patterson AFB, Ohio 45433

Brookhaven National Laboratory, ATTN: Research Library, Upton, New York 11973

Brooks Air Force Base, Radiobiology Department, Chief, San Antonio, Texas 78325

M. O. Burrell, M-RP-NIP, National Aeronautics and Space Adm., Marshall Space Flight Center, Huntsville, Alabama 35812

Walter R. Burrus, Tennecomp, Inc., P. O. Box J, Oak Ridge, Tennessee 37830

D. K. Butler, Argonne National Laboratory, 9700 South Cass Avenue, Argonne, Illinois 60439

Richard L. Childers, Physics Department, University of South Carolina, Columbia, South Carolina 25205

Maj. Anthony J. Chiota, HQ AFSC (SCTSW), Andrews AFB, Washington, D. C. 20331

R. G. Cochran, Department of Nuclear Engineering, A and M College of Texas, College Station, Texas

W. A. Coleman, Box 856, Edgewood, Maryland 21040

Ted Colvin, Bendix Systems Division, 3300 Plymouth Road, Ann Arbor, Michigan 48105

Consultant, Nuclear Medicine, Office of the Surgeon General, Washington, D. C. 20315

E. A. Cosbie, Argonne National Laboratory, Argonne, Illinois 60440

Frederick P. Cowan, Head, Health Physics Division, Brookhaven National Laboratory, Upton, L. I., New York 11973

Richard B. Curtis, Office of Research and Advanced Studies, Indiana University, Bloomington, Indiana 47401

Stanley B. Curtis, Bldg. 29, Room 213, Lawrence Radiation Laboratory, Berkeley, California 94720

Raymond Davis, Jr., Chemistry Department, Brookhaven National Laboratory, Upton, L. I., New York 11973

J. DeJuren, 3401 W. Broadway Avenue, Hawthorne, California 90250

Director, Defense Atomic Support Agency, Pentagon, Washington, D. C. 20301

Charles A. Dempsey, 6570 AMRL (MRT), Wright-Patterson AFB, Ohio 45433

Herbert DeStaebler, SLAC, Stanford University, Stanford, California 94305

Director, Defense Atomic Support Agency, ATTN: APTL, Washington, D. C. 20305

Director, Defense Atomic Support Agency, ATTN: RARP, Washington, D. C. 20305

Herman J. Donnert, U. S. Army Nuclear Defense Laboratory, AMXND-C, Edgewood Arsenal, Maryland 21010

Israel Dostrovsky, Weizmann Institute for Science, Rehovath, Israel

D. W. Drawbaugh, Westinghouse Astronuclear Laboratory, P. O. Box 10864, Pittsburgh, Pennsylvania 15236

John E. Duberg, National Aeronautics and Space Adm., Langley Research Center, Langley Field, Virginia 23365

D. L. Dye, The Boeing Company, Mail Stop S3-72, Seattle, Washington 98124

R. D. Edge, Physics Department, University of South Carolina, Columbia, South Carolina 29208

Nat Edmunson, Code R-RP-N, National Aeronautics and Space Adm., Marshall Space Flight Center, Huntsville, Alabama 35812

E. M. Finkelman, Grumman Aircraft Engineering Corp., LEM Project, Plant 25, Bethpage, L. I., New York 11714

Trutz Foelsche, National Aeronautics and Space Adm., Langley Research Center, Mail Stop 304, Langley Field, Virginia 23365

R. E. Fortney, Northrop Space Laboratories, 3401 West Broadway, Hawthorne, California 90250

Leo Fox, Code RBH, Biotechnology and Human Research Division, National Aeronautics and Space Adm., Washington, D. C. 20546

J. Y. Freeman, Division MPS, CERN, Geneva 23, Switzerland

Russell R. Galasso, Headquarters, USA Test and Evaluation Command, Aberdeen Proving Ground, Maryland 21005

J. Geibel, CERN, Geneva, Switzerland

General Dynamics/Fort Worth, ATTN: B. S. Fain and K. G. Brown, P. O. Box 748, Fort Worth, Texas 76101

R. C. Good, Jr., General Electric Company, Room 0500-VFSTC, P. O. Box 8555, Philadelphia, Pennsylvania 19101

Frederick Gordon, Jr., NASA/Goddard Space Flight Center, Code 716A, Greenbelt, Maryland 20771

Elie Gradsztajan, Institut de Physique Nucleaire, B. P. 1, 91-Orsay, FRANCE

Raymond M. Hansen, Mail Stop 235, NASA/Langley Research Center, Hampton, Virginia 23365

Harry Harrison, Code RRE, National Aeronautics and Space Adm., Hdqts., Washington, D. C. 20546

Russell Heath, Phillips Petroleum Company, P. O. Box 2067, Idaho Falls, Idaho 83401

Phillip B. Hemmig, Division of Reactor Development, U. S. Atomic Energy Commission, Washington, D. C.

Herbert D. Hendricks, NASA/Langley, Mail Stop 499, Hampton, Virginia 23365

High-Energy Preprint Library, Department of Physics, University of Toronto, Toronto 5, Ontario, CANADA

Doris M. High, Librarian, Commanding Officer, U. S. Army Nuclear Defense Laboratory, Bldg. 5695, ATTN: Library, Edgewood Arsenal, Maryland 21010

R. H. Hilberg, Bellcomm, Inc., 1100 17th Street, N. W., Washington, D. C. 20036

Charles W. Hill, Dept. 73-69, Zone 174, Lockheed-Georgia Company, Marietta, Georgia 30060

John R. Hoffman, Kaman Nuclear, 1700 Garden of the Gods Road, Colorado Springs, Colorado 80907

L. Hoffman, CERN, Geneva, Switzerland

George R. Holeman, Health Physicist, Yale University, Health Physics Division, 1136 Kline Biology Tower, 219 Prospect Street, New Haven, Connecticut 06520

J. T. Holloway, Grants and Research Contracts, Office of Space Sciences, National Aeronautics and Space Adm., Washington, D. C. 20546

Holmes and Narver, Inc., 828 South Figueroa Street, Los Angeles, California 90017

W. C. Hulten, NASA/Langley Research Center, Mail Stop 234, Hampton, Virginia 23365

H. E. Hungerford, 101 Michael Golden Laboratory, Purdue University, Lafayette, Indiana 47907

T. Inada, National Institute Radiological Sciences, 250 Kurosuna-Cho, Chiba-Shi, JAPAN

Harvey I. Israel, H-DO, Los Alamos Scientific Laboratory, P. O. Box 1663, Los Alamos, New Mexico 87544

Lt. Joseph F. Janni, WLBB, Air Force Weapons Laboratory, Kirtland AFB, New Mexico 87117

Philippe Tardy-Joubert, S.P.R., Centre d'Etudes Nucleaires de Saclay, B. P. 2, 91-Gif-Sur-Yvette, FRANCE

Clyde Jupiter, Gulf General Atomic, P. O. Box 608, San Diego, California 92112

Irving M. Karp, NASA/Lewis Research Center, 21000 Brookpark Road, Mail Stop 49-2, Cleveland, Ohio 44135

L. Katz, Director, Accelerator Laboratory, University of Saskatchewan, Saskatoon, Sask, CANADA

Glenn Keister, Boeing Airplane Company, Aerospace Division, P. O. Box 3707, Seattle, Washington 98124

J. Warren Keller, NASA Headquarters, Code RV-1, Washington, D. C. 20546

D. Aliaga-Kelly, Nuclear Enterprises Ltd., Sighthill, Edinburgh 11, SCOTLAND

James F. Kenny, Boeing Scientific Research Laboratory, P. O. Box 3981, Seattle, Washington 98124

E. C. Kidd, Zone S71, Dept. 61-2, General Dynamics/Fort Worth, P. O. Box 748, Fort Worth, Texas 76101

F. T. Kieltyka, Capt, USAF, Hq OAR (RROSP), 1400 Wilson Blvd., Arlington, Virginia 22209

E. M. Kinderman, Radiation Physics Division, Stanford Research Institute, Menlo Park, California 94025

Robert L. Kloster, McDonnell Aircraft Corp., P. O. Box 516, St. Louis, Missouri 63166

Eugene B. Konecci, Department of Management BEOB-200, University of Texas, Austin, Texas 78712

W. E. Kreger, Head, Physical Sciences Division, U. S. Naval Radiological Defense Laboratory, San Francisco, California 94135

Ed Kuhn, Nuclear Technology Corporation, 116 Main Street, White Plains, New York 10601

Pierre Lafore, Sepp, Commissariat A. L. Energie Atomique, Centre D. Etudes Nucleaires, De Fontenay-Aux-Roses (Seine), Boite Postale No. 6, 92 Fontenay Aux Roses, FRANCE

Borje Larsson, University of Uppsala, The Gustaf Werner Institute, Uppsala, SWEDEN

J. M. Lavie, Centre D. Etudes Nucleaires, De Saclay, S. E. C. R. - B. P. No. 2, 91-Gif-Sur-Yvette, FRANCE

Lawrence Radiation Laboratory, Technical Information Department, P. O. Box 808, Livermore, California 94550

Martin Leimdorfer, Industri-Matematik AB, De Geersgatan 8, Stockholm No. SWEDEN

S. H. Levine, Northrop Space Laboratories, 3401 West Broadway, 2452/61, Hawthorne, California 90250

Library, Cambridge Electron Accelerator, Harvard University, 42 Oxford Street, Cambridge, Massachusetts 02138

Library, Kaman Nuclear, 1700 Garden of the Gods Road, Colorado Springs, Colorado 80907

John R. Lilley, A-830-BBFO-78, Missile Space Systems Division, Douglas Aircraft Co., Inc., Santa Monica, California

S. J. Lindenbaum, Brookhaven National Laboratory, Upton, L. I., New York 11973

Major Russell E. Linkous, Air Force Systems Command (SCTR), Andrews AFB, Maryland 20331

M. Stanley Livingston, Cambridge Electron Accelerator, 42 Oxford Street, Cambridge, Massachusetts 02139

Lockheed Missiles and Space Co., Technical Information Center, 3251 Hanover Street, Palo Alto, California 94304

Robert Macklin, Jet Propulsion Laboratory, Pasadena, California 91103

A. Manning, Department of Physics, Valparaiso University, Valparaiso, Indiana 46383

Brian Mar, Boeing Airplane Co., MS 23-82, Aerospace Division, P. O. Box 3707, Seattle, Washington 98124

Thomas J. McGuire, ASD (ASBED-50/T. J. McGuire), Wright-Patterson AFB, Ohio 45433

E. J. McLaughlin, Space Medicine, NASA - Code MM, Washington, D. C. 20546

James E. McLaughlin, Director, Radiation Physics, U. S. Atomic Energy Commission, 376 Hudson Street, New York, New York 10014

R. V. Meghreblian, Jet Propulsion Laboratory, 4800 Oak Grove Drive, Pasadena, California 91103

Albert Metzger, Jet Propulsion Laboratory, 4800 Oak Grove Drive, Pasadena, California 91103

J. M. Miller, Chemistry Department, Columbia University, New York, New York 10027

R. A. Miller, Zone S71, Dept. 61-2, General Dynamics/Fort Worth, P. O. Box 748, Fort Worth, Texas 76101

Phillip S. Mittelman, 180 South Broadway, White Plains, New York 10605

Jerry L. Modisette, National Aeronautics and Space Adm., Manned Spacecraft Center, Houston, Texas 77001 (5 copies)

Robert B. Moler, IIT Research Institute, 10 West 35th Street, Chicago, Illinois 60616

Winnie M. Morgan, Technical Reports, Grants and Research Contracts, Office of Space Sciences, NASA, Washington, D. C. 20546 (25 copies)

B. J. Moyer, University of California, Lawrence Radiation Laboratory, 6141 Building 50A, Berkeley, California 94720

R. F. Mozley, SLAC, Stanford University, Stanford, California 94305

Frank J. Munno, Department of Chemical Engineering, University of Maryland, College Park, Maryland 20740

NASA Scientific and Technical Information Facility, ATTN: Acquisitions Branch, P. O. Box 33, College Park, Maryland 20740

R. R. Nash, Code RRM, National Aeronautics and Space Adm., Washington, D. C. 20546

W. R. Nelson, Stanford Linear Accelerator Center, P. O. Box 4349, Stanford University, Stamford, California

Keran O'Brein, U. S. Atomic Energy Commission, Health and Safety Laboratory, 376 Hudson Street, New York, New York 10014

ORED Library, Research Triangle Institute, P. O. Box 12194, Research Triangle Park, North Carolina 27709

W. K. H. Panofsky, Stanford Linear Accelerator Center, Stanford University, Stanford, California 94305

C. Passow, Institute for Experimentelle Kernphysic, der Technischen Hochschule Karlsruhe, Auf dem Kernfo Schungszentrum Karlsruhe, 75 Karlsruhe-Postfach 947, GERMANY

Wade Patterson, University of California, Lawrence Radiation Laboratory, Berkeley, California 94720

Maynard Pearson, Boeing Airplane Company, Aerospace Division, P. O. Box 3707, Seattle, Washington 98124

James A. Phillips, Los Alamos Scientific Laboratory, P. O. Box 1663, Los Alamos, New Mexico 87544

John E. Pickering, Col, USAF, NASA Headquarters, Space Medicine - Code MM, Manned Space Flight, Washington, D. C. 20546

G. F. Pieper, Code 600, National Aeronautics and Space Adm., Goddard Space Flight Center, Greenbelt, Maryland 10027

Robert Pruett, P. O. Box 95085, Los Angeles, California 90045

Radiation Effects Information Center, Battelle Memorial Institute, Columbus Laboratories, 505 King Avenue, Columbus, Ohio 43201

Arthur Reetz, Jr., NASA Headquarters, RV-1, Washington, D. C. 20546

O. Reynolds, Director, Bio-Science Programs, Office of Space Sciences, National Aeronautics and Space Adm., Washington, D. C. 20546 (5 copies)

Robert Riedesel, McConnell Douglas Astronautics Company - Western Division, 5301 Bolsa Avenue (Mail Sta. 5), Huntington Beach, California 92646

David L. Rigotti, U. S. Army Nuclear Defense Laboratory, Edgewood Arsenal, Maryland 21010

Don Robbins, ET32, National Aeronautics and Space Adm., Manned Spacecraft Center, Houston, Texas 77058

Kelvin Rooney, Atomics International, 8900 DeSoto Avenue, Canoga Park, California 91304

H. A. Sandmeier, University of California, Los Alamos Scientific Laboratory, P. O. Box 1663, Los Alamos, New Mexico 87544

J. Scanlon, Research Department, Grumman Aircraft Engineering Corp., Bethpage, New York 11714

H. J. Schaefer, U. S. Naval School of Aviation Medicine, U. S. Naval Aviation Medical Center-54, Pensacola, Florida 32512

W. Wayne Scott, Chattanooga State Technical Institute, 4501 Amnico Highway, Chattanooga, Tennessee 37401

Robert B. Seale, Department of Nuclear Engineering, University of Arizona, Tucson, Arizona 85721

W. E. Selph, LINAC, Gulf General Atomic, P. O. Box 608, San Diego, California 92112

B. S. P. Shen, Department of Astronomy, University of Pennsylvania, Philadelphia, Pennsylvania 19104

K. Shure, Westinghouse Electric Corp., Bettis Atomic Power Laboratory, P. O. Box 79, West Mifflin, Pennsylvania 15122

Robert T. Siegel, Department of Physics, College of William and Mary, Williamsburg, Virginia 23185

J. J. Singh, M. S. 234, NASA/Langley Research Center, Langley Station, Hampton, Virginia 23365

Charles Sondhaus, University of California, California College of Medicine, 1721 Griffin Avenue, Los Angeles, California 90031

Jerry Speakman, 6570 AMRL (MRBBR), Wright-Patterson AFB, Ohio

Stanford Linear Accelerator Center, ATTN: Library, P. O. Box 4349, Stanford, California 94305

William Steigelmann, Kuljian Corp., 1200 North Broad Street, Philadelphia, Pennsylvania 19121

Henry Stern, R-RP-N, NASA, Marshall Space Flight Center, Huntsville, Alabama 35812

G. R. Stevenson, Radiation Protection Group, R20, Rutherford High Energy Laboratory, Chilton, Didcot, Berkshire, ENGLAND

T. R. Strayhorn, Mail Zone 2671, General Dynamics, P. O. Box 748, Fort Worth, Texas 76101

J. A. Swartout, Union Carbide Corporation, 270 Park Avenue, New York, New York 10017

R. F. Taschek, Los Alamos Scientific Laboratory, Los Alamos, New Mexico 87544

Eizo Tajima, Rikkyo University, Ikebukuro, Toshimaku, T okyo, JAPAN

K. Tesch, DESY, Hamburg, Notkesteig 1, GERMANY

Ralph H. Thomas, Health Physics, 67 Encina Hall, Stanford University, Stanford, California 94305

O. Lyle Tiffany, Chief Scientist, Bendix Systems Division, 3300 Plymouth Road, Ann Arbor, Michigan 48103

Cornelius Tobias, University of California, Lawrence Radiation Laboratory, Berkeley, California 94720

Jacob I. Trombka, Goddard Space Flight Center, Greenbelt, Maryland 20771

W. Turchinetz, R26-411, Massachusetts Institute of Technology, Cambridge, Massachusetts 02139

Anthony Turkevich, University of Chicago, Chicago, Illinois

Werner Von Braun, Director, George C. Marshall Space Flight Center, NASA, Huntsville, Alabama 35812

G. P. Wachtell, Franklin Institute, 20th and Parkway, Philadelphia, Pennsylvania 19103

Roger Wallace, Bldg. 72, Lawrence Radiation Laboratory, Berkeley, California 94720

W. A. Wallenmeyer, Division of Research, U. S. Atomic Energy Commission, Washington, D. C. 20545

M. B. Wells, Radiation Research Associates, Inc., 1506 West Terrell Avenue, Fort Worth, Texas 76104

G. T. Western, Y-71, General Dynamics, Fort Worth, Texas 76101

Glenn A. Whan, Associate Professor, Nuclear Engineering Laboratory, The University of New Mexico, Albuquerque, New Mexico 87106

Robert V. Wheeler, R. S. Landauer, Jr., and Co., Glenwood Science Park, Glenwood, Illinois 60425

Ralph Wiley, Mail Zone Y-128, General Dynamics, Fort Worth, Texas 76101

Maurice Wilkinson, The Boeing Company, M. S. 23-82, Seattle, Washington 98124

William E. Wilson, Jr., Reactor Supervisor, Department of Nuclear Engineering, Nuclear Reactor Bldg., University of Washington, Seattle, Washington 98105

W. R. Yucker, A-2-833, Douglas Aircraft Co., Nuclear Department, 3000 Ocean Park Boulevard, Santa Monica, California 90405

Marcello Zocchi, Reactor and Radiation, National Bureau of Standards, Washington, D. C. 20234

K. Ziock, Department of Physics, University of Virginia, Charlottesville, Virginia 32901

Walter Schimmerling, Head, Radiations Measurements Group, Princeton-Pennsylvania Accelerator, P. O. Box 682, Princeton, New Jersey 08540

ORNL-TM-2253

Internal Distribution

1- 3. L. S. Abbott
4. R. G. Alsmiller, Jr.
5. G. T. Chapman
6. C. E. Clifford
7. G. de Saussure
8- 9. F. C. Maienschein
10. R. W. Peelle
11. F. G. Perey
12. R. T. Santoro
13. D. Sundberg
14. D. K. Trubey
15-29. J. W. Wachter
30. W. Zobel
31. E. R. Cohen (consultant)
32. B. C. Diven (consultant)
33. W. N. Hess (consultant)
34. M. H. Kalos (consultant
35. L. V. Spencer (consultant)
36-37. Central Research Library
38. ORNL Y-12 Technical Library
Document Reference Section
39-40. Laboratory Records Department
41. Laboratory Records ORNL RC
42. ORNL Patent Office

External Distribution

43-57. W. R. Burrus, Tennecomp, Oak Ridge, Tennessee 37830
58-72. W. A. Gibson, Tennecomp, Oak Ridge, Tennessee 37830
73. C. F. Johnson, General Dynamics, Fort Worth, Texas
74-288. Given NASA Space Shielding and AEC High-Energy Accelerator Shielding Distribution as shown on preceding pages
288-302. Division of Technical Information Extension (DTIE)
303. Laboratory and University Division (ORO)